This is to certify that the
thesis entitled

Z-SOURCE INVERTER CONTROL FOR TRACTION DRIVE OF
FUEL CELL – BATTERY HYBRID VEHICLES

presented by

Kent Daniel Holland

has been accepted towards fulfillment
of the requirements for the

M.S. degree in Electrical Engineering

Major Professor's Signature

Aug. 26, 2005

Date

Z-SOURCE INVERTER CONTROL FOR TRACTION DRIVE OF FUEL CELL – BATTERY HYBRID VEHICLES

By

Kent Daniel Holland

A THESIS

Submitted to
Michigan State University
in partial fulfillment of the requirements
for the degree of

MASTER OF SCIENCE

Department of Electrical and Computer Engineering

2005

ABSTRACT

Z-SOURCE INVERTER CONTROL FOR TRACTION DRIVE OF FUEL CELL – BATTERY HYBRID VEHICLES

By

Kent Daniel Holland

Abstract— This paper presents a Fuel Cell Vehicle (FCV) control strategy using the Z-source inverter to control power from the fuel cell, power to the traction motor, and State of Charge (SOC) of the battery. The recently presented Z-source inverter is well suited for many applications, including FCVs. The Z-source inverter utilizes an exclusive Z-source (LC) network to link the main inverter circuit to the fuel cell (or any dc power source). A new concept is revealed that substitutes a high voltage battery for one (or both) of the capacitors from the Z-source network. By controlling the shoot-through duty cycle we can control the battery voltage (thus controlling SOC) therefore there is no need for a separate dc-dc converter. By controlling the shoot-through duty cycle and modulation index we can produce any desired output ac voltage (thus there is no need for a dc-dc boost converter), regulate battery SOC, and control FC output power (or voltage) simultaneously. The Z-source inverter has the benefit of enhanced reliability due to the fact that momentary shoot-through can no longer destroy the inverter (i.e. both devices of a phase leg can be on for a significant period of time).These facts make the Z-source inverter highly desirable for use in hybrid electric vehicles, as the cost and complexity is greatly reduced when compared to traditional inverters. Although the Z-source inverter could be utilized in any HEV, this paper presents the control strategy and demonstrates these features for use in a FCV. These new concepts will be demonstrated by simulation and experimental results.

Dedicated to my Mother

Anja Kaarina Turkki

December 26, 1943 – March 28, 2004

ACKNOWLEDGEMENTS

I first wish to thank my Sister Dr. Karina Holland, congratulations for being the first doctor in our entire family. I also wish to thank my Mother, I know how proud she was of our academic accomplishments, I wish she could be there to see us graduate again. My biggest thanks goes to my Father, who motivated me to start and continue my education, and also to find direction in education. By his teaching me love and respect for the great outdoors and the environment, it was easy for me to choose to apply my education towards alternative vehicles, so that I would make a difference, and protect the environment that we all take for granted.

I also wish to thank my advisor Dr. Peng, and to all that work in his lab at Michigan State University, thank you for all the help and sharing your knowledge.

TABLE OF CONTENTS

LIST OF TABLES

LIST OF FIGURES

KEYS TO SYMBOLS OR ABBREVIATIONS

Hybrid electric vehicle (HEV)

Internal combustion engine (ICE)

Electric vehicle (EV)

Zero emission vehicle (ZEV)

Hybrid vehicle (HV)

Fuel cell (FC)

Fuel cell vehicle (FCV)

Fuel cell hybrid electric vehicle (FC HEV)

Pulse width modulation (PWM)

Sinusoidal pulse width modulation (SPWM)

Modulation index (M)

Boost factor (B)

Voltage gain (MB)

Phase A voltage reference (V_a)

Phase B voltage reference (V_b)

Phase C voltage reference (V_c)

Upper shoot-through envelope (V_p)

Lower shoot-through envelope (V_n)

Time during shoot through (T_0)

Switching cycle interval (T)

Output ac voltage ($\hat{v}_{ac}$)

Input dc voltage (V_0)

Peak dc-link voltage across the inverter bridge ($\hat{v}_i$)

Buck–boost factor (B_B)

Capacitor voltage (V_C)

Switching Device Power (SDP)

Constant power speed ratio (CPSR)

Shoot-through duty cycle (D_0)

Battery terminal voltage (Vb)

State of charge (SOC)

Phase A upper switch gate control signal (S_{ap})

Phase A Lower switch gate control signal (S_{an})

Phase B upper switch gate control signal (S_{bp})

Phase B Lower switch gate control signal (S_{bn})

Phase C upper switch gate control signal (S_{cp})

Phase C Lower switch gate control signal (S_{cn})

Upper shoot-through envelope reference signal (V_{pref})

Lower shoot-through envelope reference signal (V_{nref})

1. INTRODUCTION

Hybrid electric vehicles (HEVs) have recently become attractive for many reasons. The U.S. government is interested in becoming less dependant on foreign oil reserves. Not to mention that these oil reserves are being rapidly depleted. The typical consumer is interested in achieving greatly increased fuel efficiency, while maintaining the performance and conveniences offered by conventional gasoline powered vehicles. Environmentalists, consumers, and government alike are all interested in decreased tailpipe emissions [1]. These emissions contain greenhouse gases and other pollutants that are harmful to humans and thought to be the major cause of global warming [2]. Due the recent increased gas prices, and the need for reduced emissions and increased efficiency, the timing for HEV development could not be better.

1.1 Conventional Vehicles

The conventional vehicle uses an internal combustion engine (ICE), which supplies mechanical power to the wheels, as shown in figure 1. One problem associated with conventional ICE vehicles is that the typical driver demands quick acceleration, which in turn requires a more powerful, less efficient engine. The problem is that most of the time only a small part of the power is used, however the larger engine is always unnecessarily guzzling gas. Larger engines use more gas because they are heavier, the displacement of the cylinders is larger, and they usually have more cylinders [3]. The problem with smaller engines is they may not be able to keep up with traffic as well, especially when traveling uphill. While millions of automobiles are sold every year, it is clear that some alternative to the conventional vehicle must be developed.

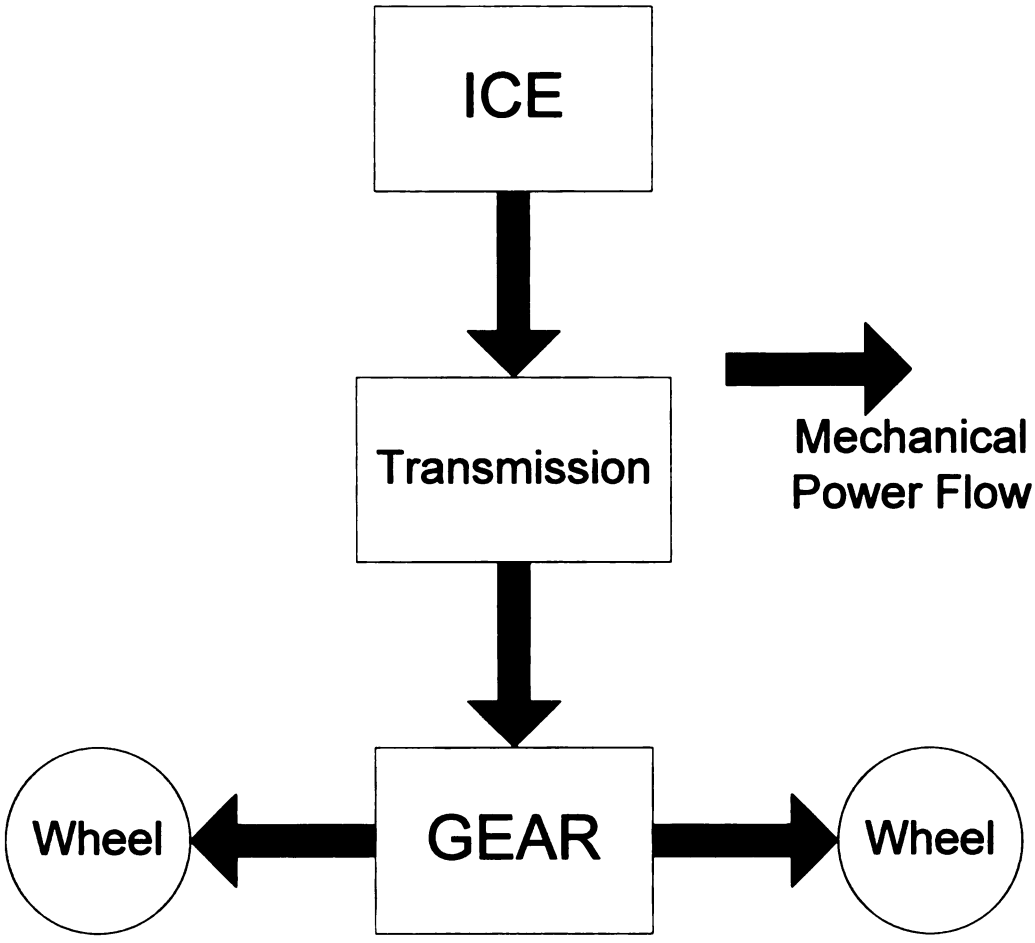

Figure 1. Typical Internal Combustion Engine (ICE) Vehicle

One possible alternative is the conventional electric vehicle (EV). The EV uses batteries to store and supply electric power to the motor, as shown in figure 2. The main advantage of the EV is that it is a zero emission vehicle (ZEV). Although there is some pollution created when the electricity is generated at the power plant, this is insignificant compared to emissions from conventional ICE vehicles. EVs are also very efficient when compared to conventional ICE vehicles, only about 20% of the chemical energy in gasoline is converted into work at the wheels of an ICE vehicle, 75% or more of the energy from a battery reaches the wheels of an EV [4]. EVs also provide strong

performance, due to the fact that electric motors provide nearly peak power even at low speeds. However the cost, performance, and convenience of an EV all depend on the battery. There are several types of batteries commonly used in EVs, advanced lead-acid batteries, nickel-metal hydride, and lithium polymer batteries [4]. Even the best of these batteries can store only a limited amount of energy, thus the range of EVs is still limited. Recharging the batteries is also a problem, although home recharging systems are available, recharging sites away from home are scarce, and the time required to charge the batteries can be substantial. While the EV is very promising, currently the drawbacks outweigh the benefits, and much work needs to be done to make the EV a realizable solution.

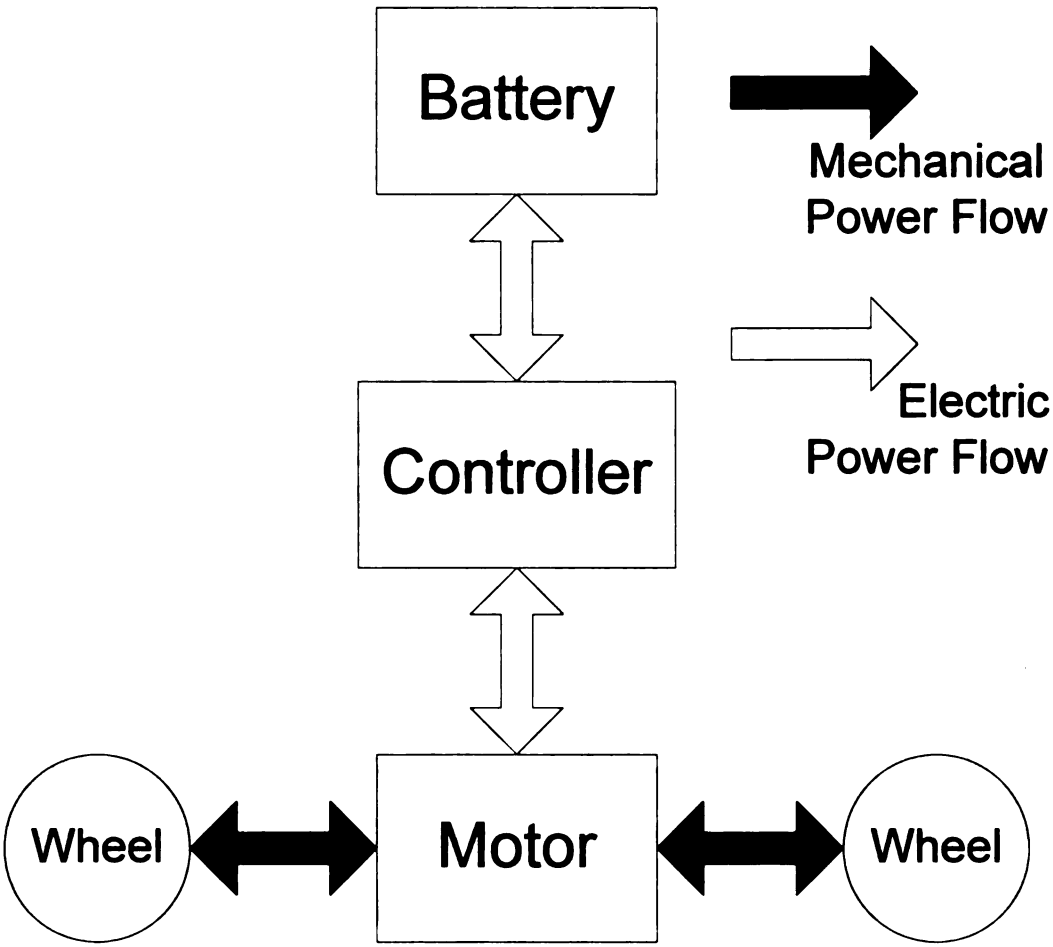

Figure 2. Typical Electric Vehicle (EV)

1.2 Hybrid Vehicles

Currently the most feasible alternative to the conventional vehicle is a hybrid vehicle (HV). A HV combines two or more power sources in attempt to gain greater overall vehicle efficiency and reduced emissions. There are many types of HVs, and until recently they have mainly been large vehicles such as busses, trains, and submarines. Another more familiar example of a HV is a motorized pedal bike, which combines the power from a small electric or gas motor along with power from the rider legs. In fact any vehicle that combines two or more power sources that provide energy for propulsion, directly or indirectly, is a HV.

A hybrid electric vehicle (HEV) combines an EVs energy storage system, along with an energy source, typically an ICE. The HEV can achieve greater overall efficiency through the use of regenerative braking. During regenerative breaking an electric motor acts like a generator, using the wheels to apply torque to the motor to generate electrical power, this torque in turn slows the vehicle down. The energy created during regenerative braking is stored in the battery until needed. Electrical storage systems commonly include batteries, ultra capacitors, or combinations of these. Another energy saving benefit of a HEV is that the power sources can be optimally controlled such that each source operates efficiently. For example a typical HEV incorporates a smaller more efficient ICE compared to a conventional vehicle. When more power is needed than the ICE can provide, as in acceleration or uphill travel, the battery delivers the extra needed power. The ICE may be alternative fuel, such as bio-diesel, methanol, natural gas, or alternatives to the ICE such as solar panels, and fuel cells.

1.2.1 Series Hybrid Vehicle

HVs can have several different configurations, and many types of power sources. The series HEV typically uses an ICE to mechanically turn a generator which supplies electric power to the electric traction motor, while excess power is stored in a battery or ultra-capacitor, as shown in figure 3. Thus the series HEV can be thought as an EV with an on board battery charger. This configuration allows the ICE to operate at a maximum point of efficiency. The ICE runs for extended periods of time at maximum efficiency, and shuts off when the batteries reach full charge. This also allows the engine size to be minimized to just satisfy the average power requirements. Also because there are less mechanical connections, simple packaging and modularization can be achieved.

There remain several problems with the series HEV. First the electric motors and power electronics need to be sized to provide all of the power to the road, thus the propulsion system tends to be more expensive. The efficiency of a series HEV also suffers due to the number of energy conversions, in the form of chemical energy to mechanical energy to electrical energy back to mechanical energy. Another major issue is battery life, the batteries available today cannot last for the vehicles expected life, because of the large number of rapid charge, and deep discharge cycles that they must withstand during daily driving [4]. In the future it is likely that battery technology will advance rapidly, and the cost and efficiency of propulsion systems will decrease, which will make the series HEV more realizable.

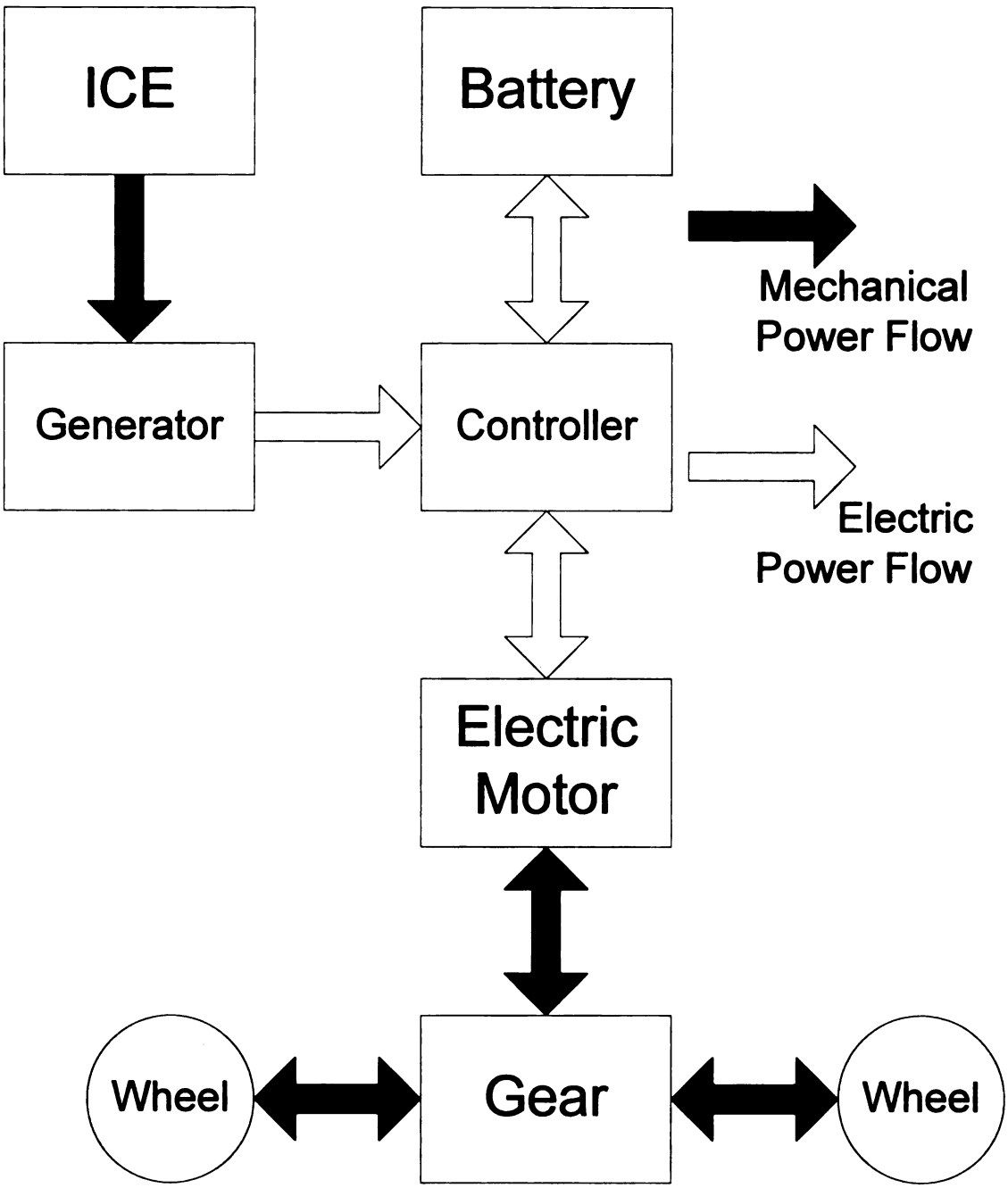

Figure 3. Typical Series HEV [5]

1.2.2 Parallel Hybrid Vehicle

Another common HV configuration is the parallel HV. In the parallel HEV both the ICE, and the electric motor can independently propel the vehicle or assist each other, as seen in figure 4. Also the ICE can power the vehicle and recharge the battery using the motor as a generator. The parallel HEV has several main advantages over the conventional ICE vehicle, and the series HEV. First in the energy conversion efficiency, the mechanical connection between the ICE and the wheels reduces the amount of power conversion from the main energy source. Second the engine and electric motor sizes can be decreased because of the fact that both can supply power to the wheels simultaneously. This results in increased fuel economy and reduced pollutant emissions. However the benefits of a smaller ICE and electric motor may be offset by the requirement of a complex transmission [4].

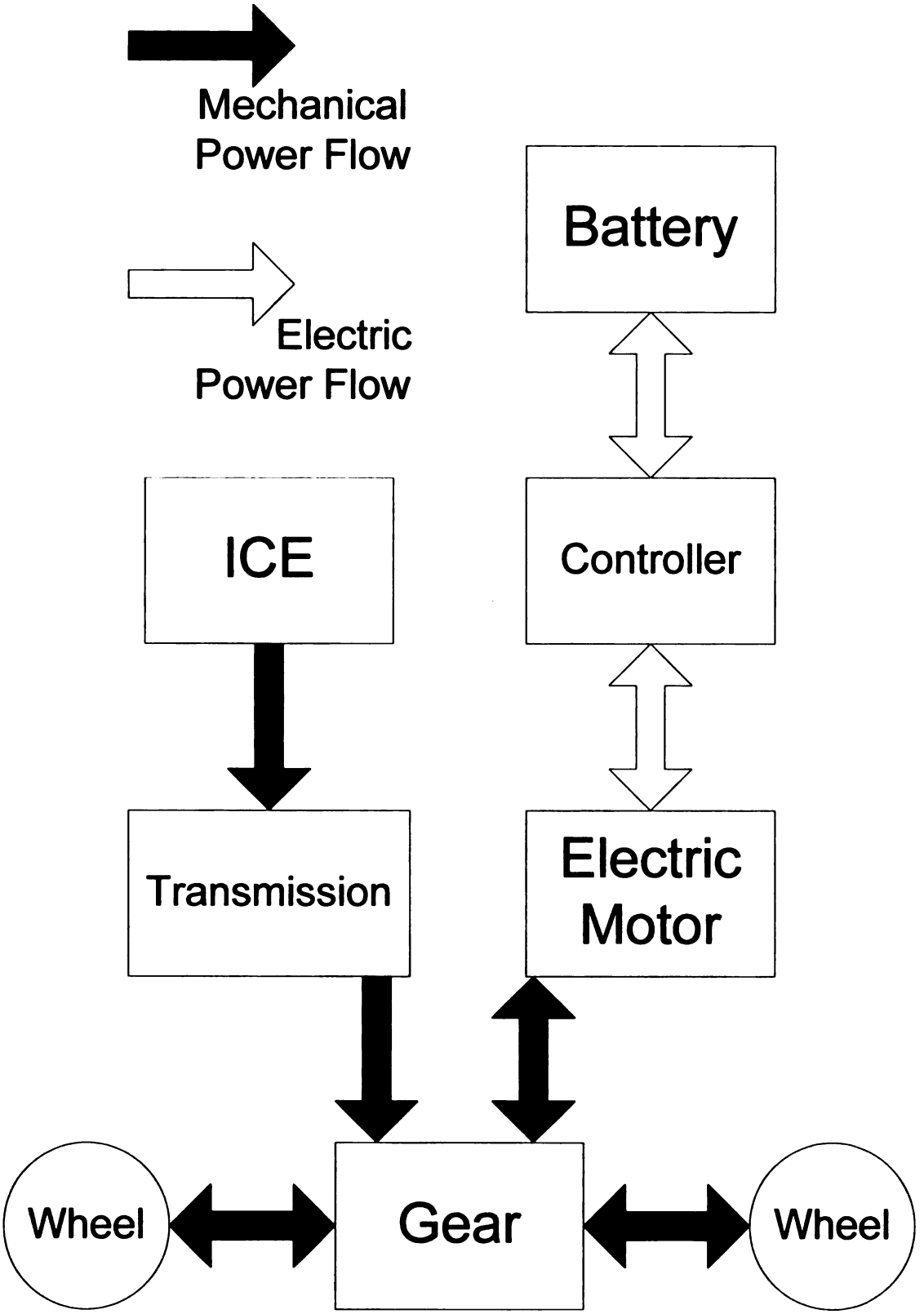

Figure 4. Typical Parallel HEV [5]

1.2.3 Series-Parallel Hybrid Vehicle

Series HEVs and parallel HEVs can be combined in different ways, commonly referred to as series-parallel HEVs [5]. In the series-parallel type of hybrid, there are several possible ways to operate the vehicle, series, parallel, or some combination of both, which utilizes the advantages of both configurations. Depending on the driving conditions, the most advantageous operating mode could be selected. The main drawback is that this configuration suffers from a more complicated structure, and higher cost than either a series or a parallel does.

Although several automobile companies now have HEVs on the market, it has been proven difficult to sell cars that cost more, but to the average consumer does not offer significant and obvious advantages. Experts rank hybrid electric vehicles only as a temporary solution, before the fuel cell cars and the hydrogen infrastructure are generally available [6].

1.3 Fuel Cell Vehicles

Fuel cells have achieved global attention as an alternative power source for HEVs. Fuel cell vehicles (FCVs), are being developed by auto manufacturers, and have generated interest among industry, environmentalists and consumers. A FCV promises the air quality benefits of a battery-powered electric vehicle, with the driving range and convenience of a conventional ICE vehicle. The fuel cell is capable of producing energy from fuels like hydrogen, methanol, or gasoline, without combustion, or conversion to mechanical energy between. When using hydrogen as a fuel, the only exhaust will be water in theory. This technology promises to make use of the advantages of the electric vehicle drive train without being restricted to short range. Figure 5 shows the typical Fuel cell hybrid electric vehicle (FC HEV), which consists of the fuel cell, controller, battery

(optional) and electric motor [7].

FCVs with regenerative braking and energy storage are clearly the best solution to provide low (possibly zero) emissions, and long range. However technology is not ready to combine all promising advantages of fuel cells in one affordable system, and the infrastructure (i.e. refueling stations) for hydrogen needs to be established. The FCV appears to be the most reasonable solution for the not to distant future, as the cost of a fuel cell is reduced, and the hydrogen infrastructure is built.

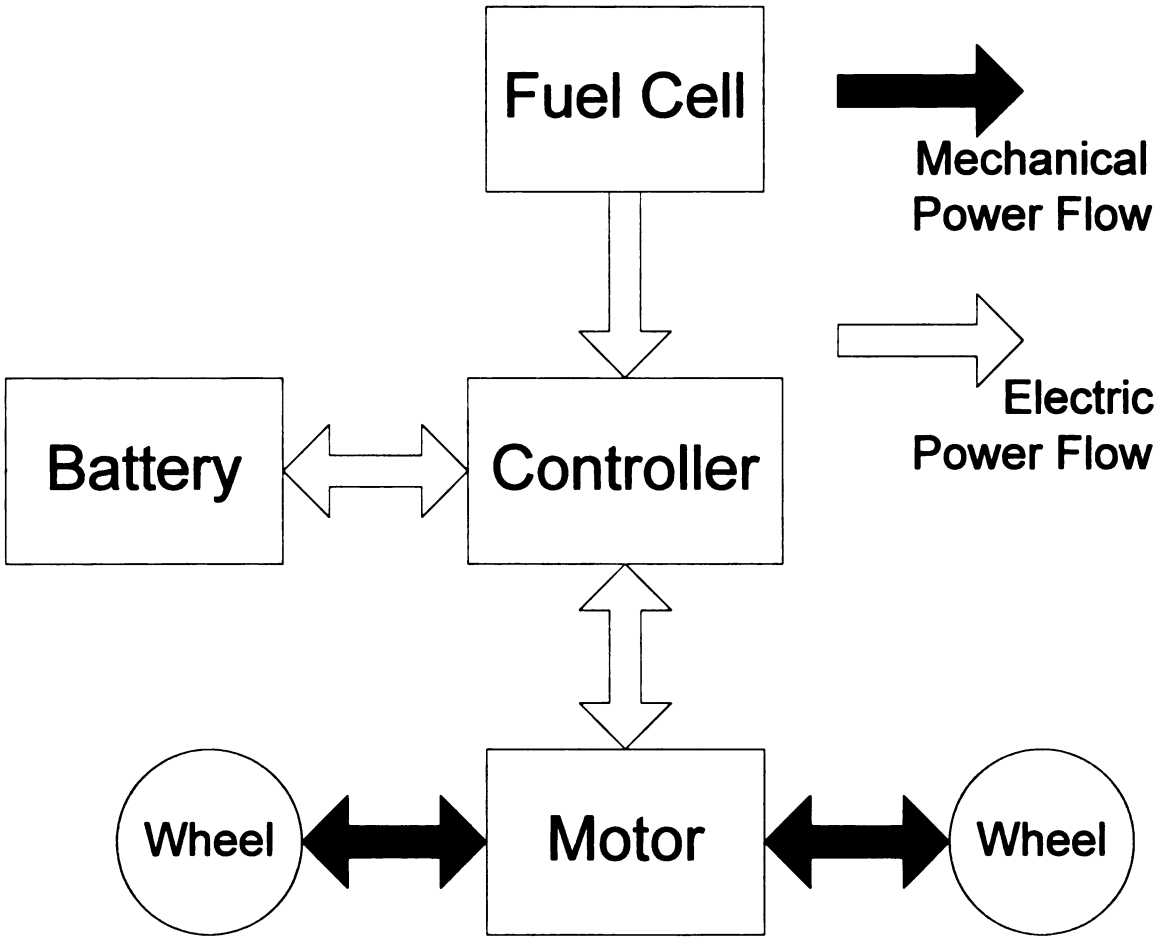

Figure 5. Typical Fuel Cell Vehicle [7]

1.4 Outline of Thesis

The goal of this research is to develop a prototype of a FCV drive train using the Z-source inverter. In addition it will be shown that the Zsource inverter can be used for control of the fuel cell power, battery state of charge (SOC), and traction drive. The major contributions of this work towards this goal are:

Chapter 2: Reviews the current FCV power electronics technologies, and introduces their control strategies. The Zsource inverter and its control strategies are also introduced.

Chapter 3: Compares the Zsource inverter to the current FCV power electronics technologies.

Chapter 4: Provides an introduction to FCV operating modes. Current FCV technology will also be presented.

Chapter 5: Will demonstrate that the Zsource inverter can indeed provide the above mentioned goals, by computer simulations.

Chapter 6: Will further demonstrate that the Zsource inverter can achieve these goals, and that the Zsource inverter can be implemented in a FCV, through the use of experiments.

2. FUEL CELL VEHICLE POWER ELECTRONICS REVIEW

FCVs employ an inverter to control the dc power from the fuel cell and battery and convert the dc power into ac power to be delivered to the motor. In this chapter the power electronics for a FCV will be discussed. Starting with two traditional inverter topologies, the voltage source and current source inverters, and finally the Zsource inverter will be introduced.

2.1 Voltage Source Inverter

Traditionally there have been two inverter topologies; voltage source inverters, and current source inverters. The voltage source inverter as seen in figure 6 consists of a dc voltage source, a large dc-link capacitor, and a three phase bridge inverter, which consists of six semiconductor switching devices. The voltage on the dc side is smoothed by a capacitor, while the current on the dc side is unsmoothed (contains an ac ripple) [8].

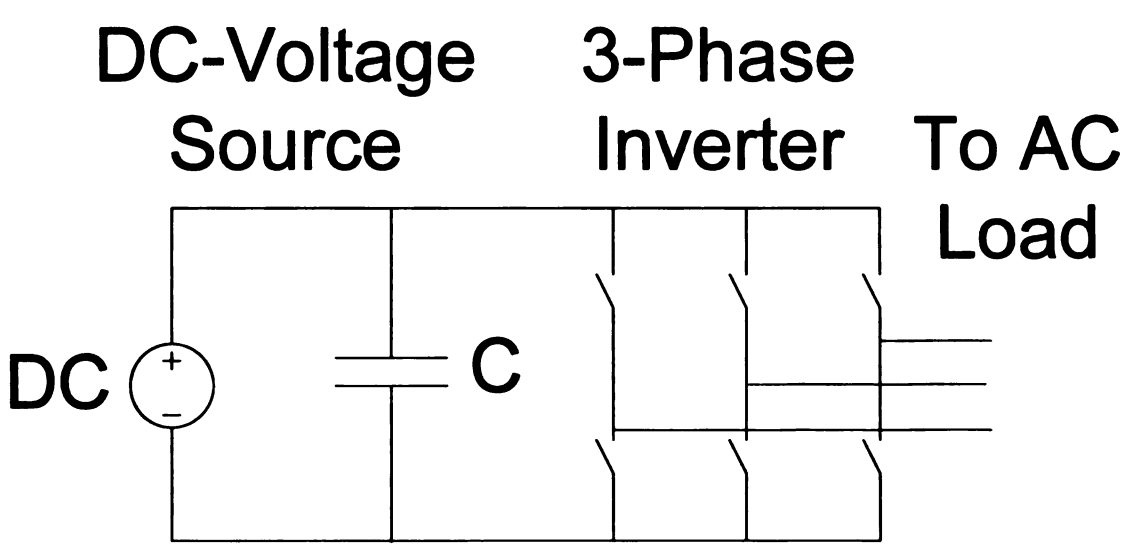

Figure 6. Traditional voltage source inverter

The voltage source inverter is the most commonly used inverter, however it suffers from the following problems. The output ac voltage is limited to below the dc voltage, therefore an additional dc-dc boost (step-up) converter is needed to obtain an output ac voltage greater than the dc voltage source [10]. This additional dc-dc converter will increase the cost and complexity of the system, as well as lowering the systems efficiency. The voltage source inverter's reliability also suffers from the problem of shoot through. Obviously, both devices in any phase leg can never be on simultaneously because the short circuit would cause huge currents to flow and damage the switching devices.

2.1.1 Voltage Source Inverter Circuit Analysis

To familiarize the reader to the operation of the voltage source inverter, a single phase half-bridge inverter, as shown in figure 7, will be examined.

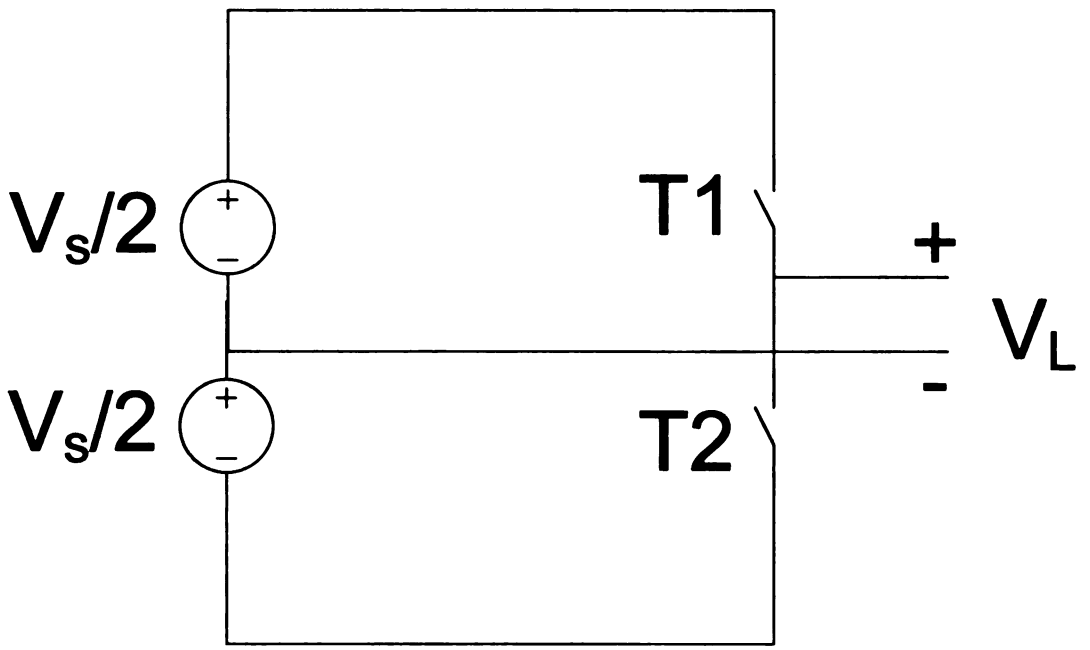

Figure 7. Single phase half-bridge inverter

When transistor T1 is ON, a voltage Vs/2 will be applied to the load. Similarly, if T2 is ON -Vs/2 will be applied to the load. Thus the inverter generates the voltages + Vs/2 or - Vs/2 at the load. The inverter switches can be digitally controlled in such a way that the voltages generated at the output can represent an ac sinewave.

A three phase inverter, such as the one shown in figure 6, can be constructed from three single phase half-bridge inverters in parallel [11]. The output ac voltages are displaced 120 degrees relative to each other, in order to achieve three phase balanced operation.

2.1.2 Voltage Source Inverter Control

Many pulse width modulation (PWM) control methods have been developed and used for the traditional 3-phase voltage source inverter. The traditional V-source inverter has six active vectors (or switching states) when the dc voltage is impressed across the load and two zero vectors when the load terminals are shorted through either the lower or upper three devices. These total eight switching states and their combinations have spawned many PWM control schemes.

Typically conventional PWM methods are applied to control the voltage source inverter. Conventional PWM can be achieved using a simple pulse width modulator, as shown in figure 8. The pulse width modulator produces a logic signal, referred to as sinusoidal PWM (SPWM), that is used to command the inverters power transistors to turn on (saturated) and off (cutoff), in such a way as to produce a sine wave at the inverters output. As figure 8 shows a simple pulse width modulator can be implemented using a comparator. The comparator is used to compare a reference signal, V_{ref}, and a carrier signal, $V_{carrier}$. The comparator produces a logic-level output as shown in figure 9, which

is logic-high whenever V_{ref} is greater than $V_{carrier}$, and logic-low whenever V_{ref} is less than $V_{carrier}$ [12]. This output is used to control the upper switch in a phase leg. To control the lower switch the signal is inverted.

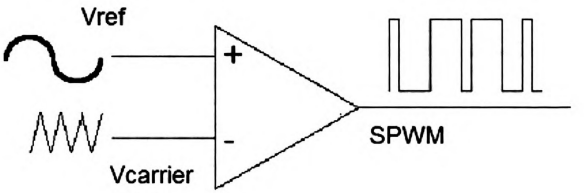

Figure 8. Simple pulse width modulator [12]

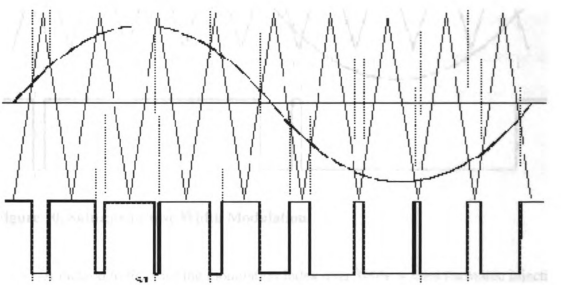

Figure 9. SPWM generation

The amplitude of the inverters output is controlled by the modulation index, which is V_{ref} divided by $V_{carrier}$ [11]. Obviously if the amplitude of V_{ref} is controlled, the modulation index is controlled, and the amplitude of the inverters output is controlled.

The modulation index of the waveforms shown in figure 9 is around .8. If the amplitude of V_{ref} (sinewave) is decreased, the modulation index is decreased, the PWM will spend less time at the logic-high state, and the average of the output signal will be decreased. If the amplitude of V_{ref} is increased, the modulation index is increased, the PWM will spend more time at the logic-high state, and the average of the output signal will be increased. Using this simple pulse width modulator the maximum modulation index is one, or 100%, that is V_{ref} can never exceed $V_{carrier}$ or the linear relationship between V_{ref} and the average output signal will be lost [13], as shown in figure 10.

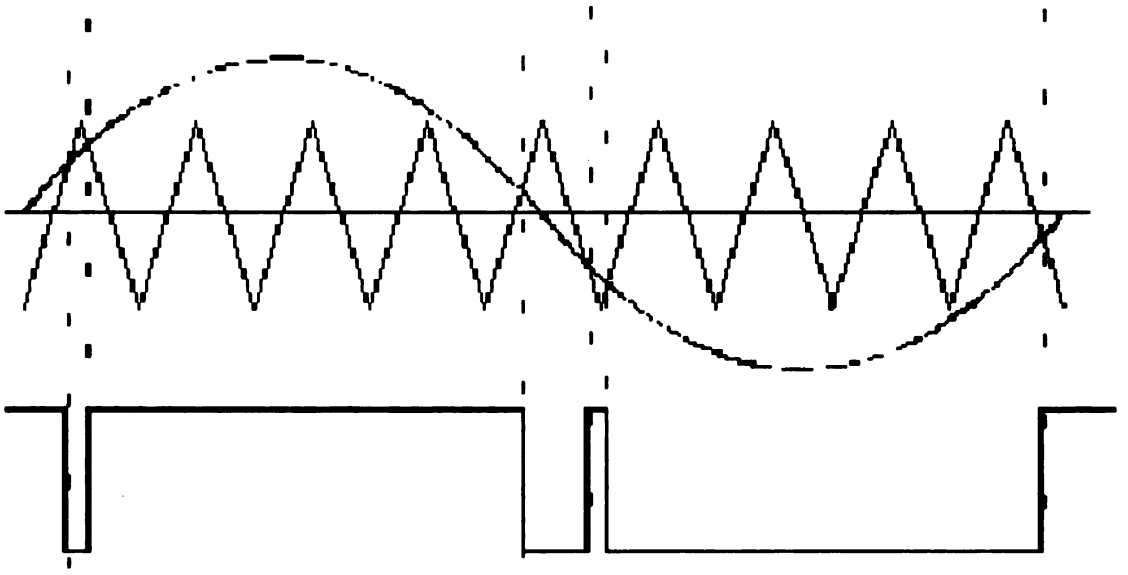

Figure 10. Saturated Pulse Width Modulation

A method to increase the modulation index over 100% is third harmonic injection. Basically third harmonics are added to V_{ref} which flattens the top of the resulting signal, allowing the amplitude of V_{ref} to be turned up higher than $V_{carrier}$. Which allows the modulation index to be increased greater than one, thus the PWM will spend more time at the logic-high state, and the average of the output signal will be increased.

The maximum available voltage on a motor using a standard three-phase power

inverter is around 86% of the dc link voltage [14]. Figure 11 shows the standard sinewave reference signal, which can achieve 100% (of $V_{carrier}$) maximum modulation index. Adding third harmonics to V_{ref} decreases the overall amplitude of the resulting reference signal, that is the resulting reference signal never reaches either 0% or 100% (of $V_{carrier}$), Figure 12. This is due to the fact that the minimum of the 3rd harmonic corresponds to the maximum of the fundamental and vice versa. This allows the fundamental signal amplitude to be increased up to the point were the modified modulating signal reaches the 100% limit of $V_{carrier}$, as shown in Figure 13. By applying an appropriate coefficient to the third harmonic component, which is 1/6 of the fundamental [15], the fundamental amplitude can be increased by 15%.

When considering a balanced three phase system, the third harmonic components are cancelled out, because a 120-degree phase-shift on the fundamental corresponds to a 360-degree shift for the third harmonic, thus there are sinusoidal voltages (and therefore currents) on the motor windings, and line to line voltage is 15% higher than with pure sinewave PWM modulation [14].

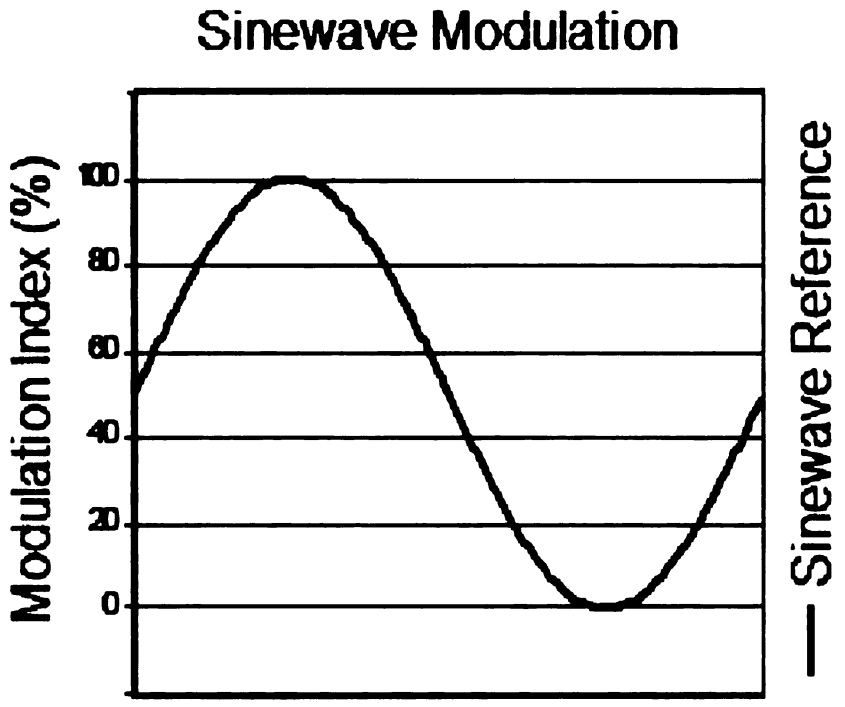

Figure 11. Standard sinewave reference signal at 100% modulation index [14]

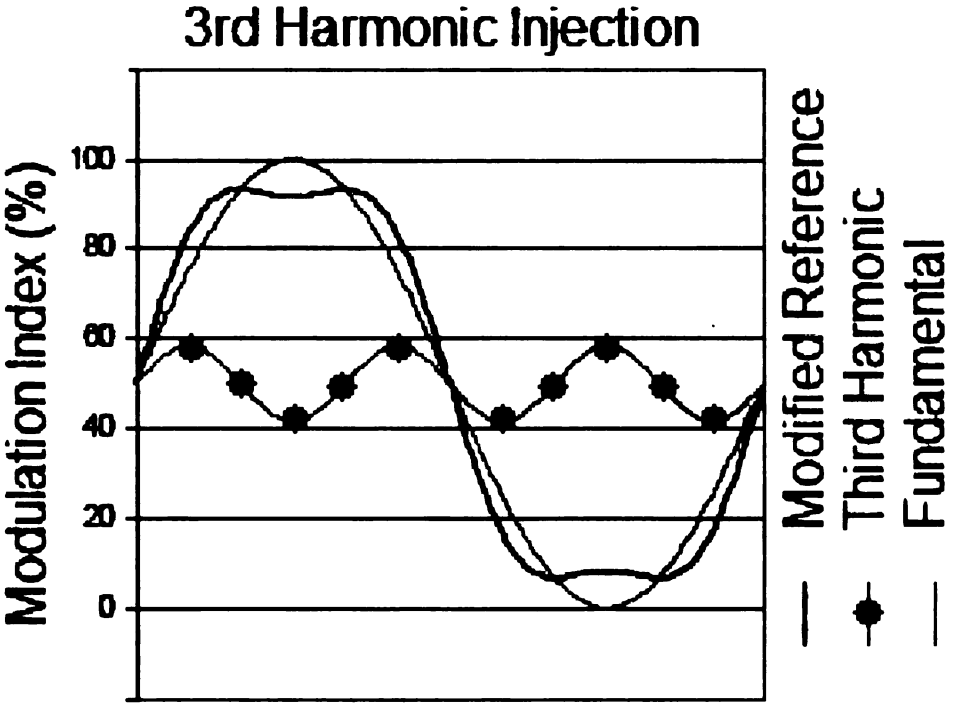

Figure 12. Reference signal modified with third harmonics, equivilant to standard sinewave reference signal at 100% modulation index [14]

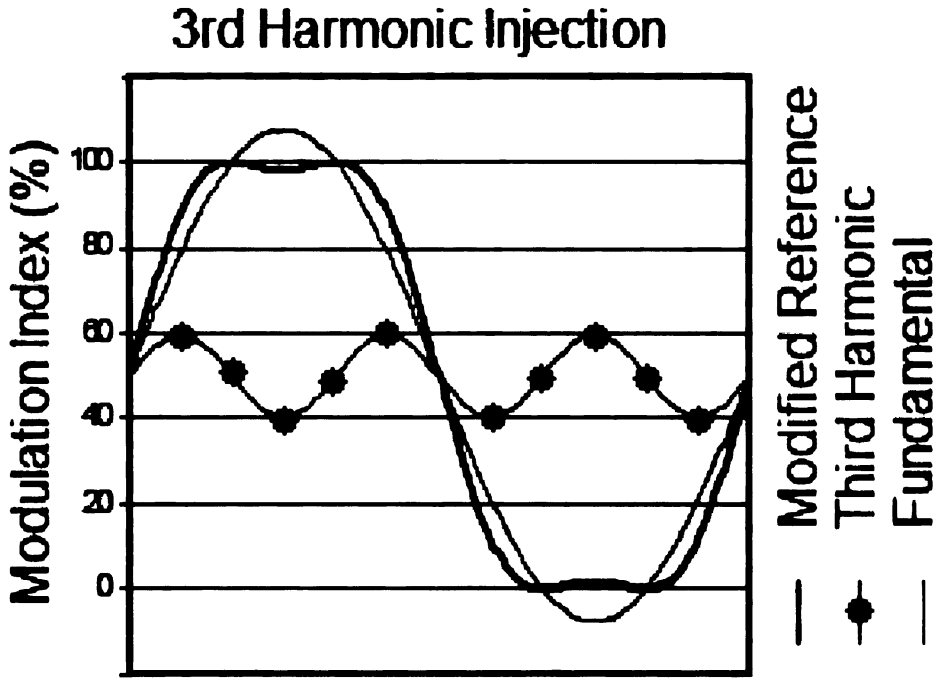

Figure 13. Reference signal modified with third harmonics at 100% modulation index [14]

The reference signals frequency controls the desired output frequency, the carrier signals frequency is many times higher and determines the inverter switching frequency (speed at which the inverters power transistors to turn on and off). The reference signal can be recovered from the inverters output SPWM by low pass filtering.

2.2 Current Source Inverter

The traditional current source inverter is shown in figure 14. The current source inverter typically consists of a large dc inductor fed by a dc voltage source (together these are the current source), and a three phase bridge inverter. The current on the dc side is smoothed by an inductance, while the voltage on the dc side is unsmoothed (contains an ac ripple) [8].

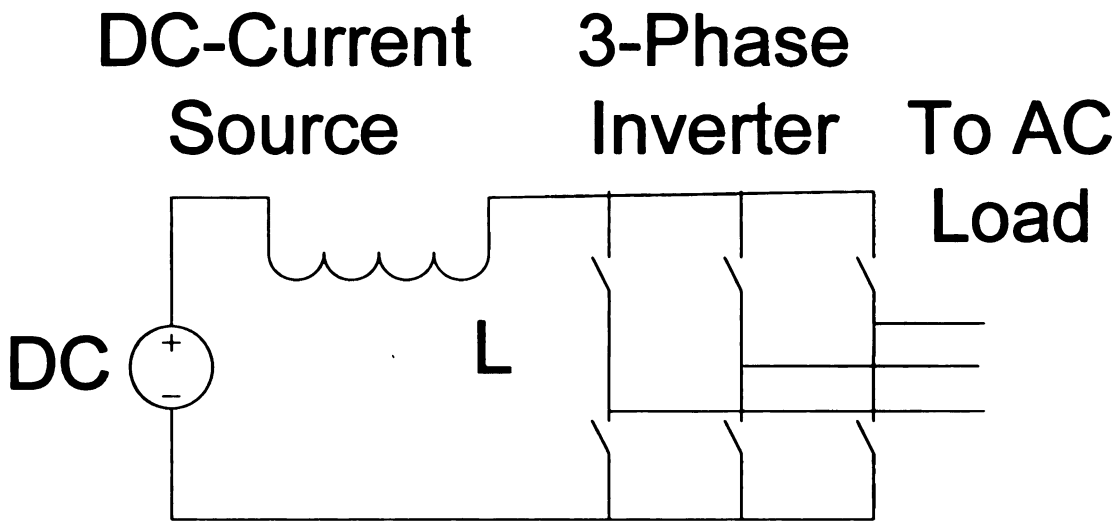

Figure 14. Traditional current source inverter

The current source inverter suffers from the following problems. The output ac voltage has to be above the dc input voltage, thus an additional dc-dc buck (step-down) converter is needed to obtain an output ac voltage less than the dc input voltage. This additional dc-dc converter will increase the cost and complexity of the system, as well as lowering the efficiency. The current source inverter's reliability also suffers from the problem of an open circuit. That is, at least one upper switch and one lower switch must always be on [11]. That is because the inductors current cannot change instantaneously, the inductor current would momentarily continue to flow through the switching devices, which have high resistance in the off state, obviously this would cause a huge voltage spike across the switching devices, which would damage or destroy the switching device.

2.3 Zsource Inverter

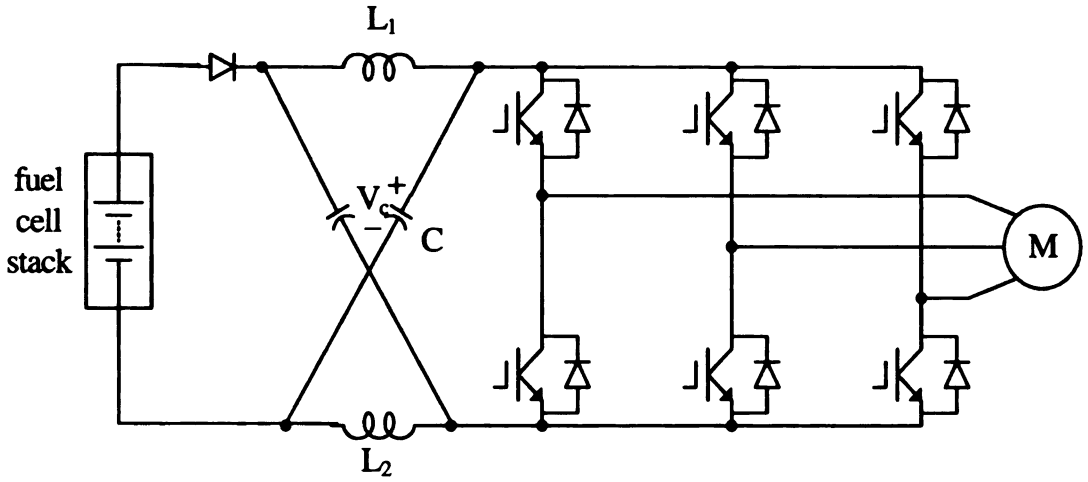

Figure 15. Zsource inverter for a FCV

Figure 15 shows the Zsource inverter for a FCV. The Zsource inverter utilizes an impedance network (Z network) to link the main inverter circuit to the fuel cell (or any dc power source). This impedance network provides unique features and advantages over the traditional inverters. The impedance network consists of two capacitors connected in an X fashion, and two inductors, to save space a split core inductor can be used. Although the Zsource inverter can be used for many applications, including dc-ac, ac-dc, ac-ac, dc-dc power conversions, with any ac or dc source and load, this thesis will focus on a Zsource inverter for a fuel cell vehicle. That is, for dc-ac power conversion with a fuel cell as the dc power source, and a motor for the ac load.

The Z-source inverter advantageously utilizes the shoot-through states to boost the dc bus voltage by gating on both the upper and lower switches of a phase leg. Figure 16 shows the schematic of the Z-source network during the shoot-through state. Obviously the capacitor voltage is boosted during this state. This is because the current

ramps up through the inductors, whose voltages are $V_L = L\,di/dt$. Thus inductor voltage increases, due to the increasing current. The capacitors are in parallel with the inductors during this state, therefore the capacitor voltage is also increased, which boosts the dc link voltage during the nonshoot-through states. Therefore, the Z-source inverter can buck (by lowering the modulation index) and boost voltage to a desired output voltage that is greater than the available dc bus voltage. In addition, the reliability of the inverter is greatly improved because the shoot-through can no longer destroy the circuit. Thus it provides a low-cost, reliable, and highly efficient single-stage structure for buck and boost power conversion.

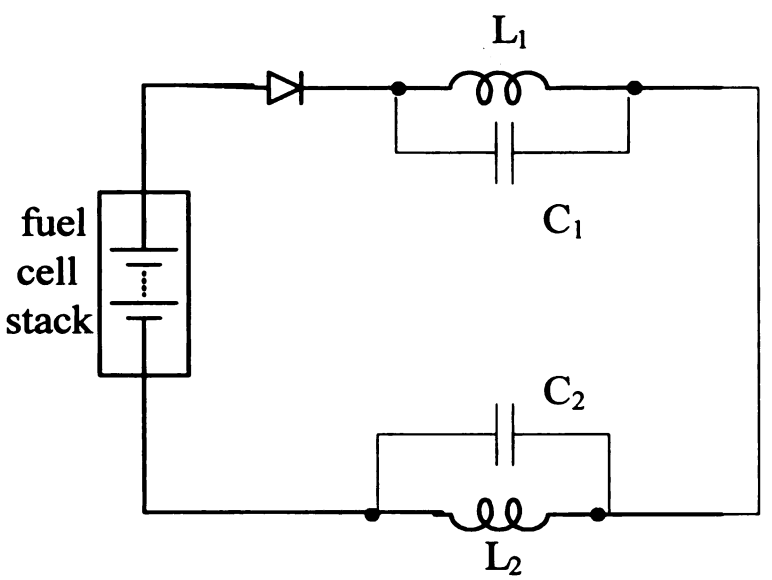

Figure 16. Z-source network during the shoot-through state

2.4 Zsource Inverter Control

Conventional pulse width modulation (PWM) methods can be applied to control the Zsource inverter. The difference between the conventional PWM as previously explained for the voltage source inverter, and the PWM used to control the Zsource, is

that the shoot through zero state is introduced into the PWM. The shoot through zero state is produced when two switches in any phase leg are both gated on, causing a short circuit across the Z network. This shoot through zero state is forbidden in the traditional voltage source inverter, because it would damage or destroy the switching device. The shoot through zero state provides the Zsource inverter the ability to boost (step up) the dc bus voltage, by boosting the capacitor voltage, as previously explained. This boosting of the dc bus voltage obviously can be used to increase the output ac voltage. Clearly the Zsource inverter has the ability to buck (step down) the output ac voltage by lowering the modulation index. So a great advantage of the Zsource inverter is revealed, the Zsource inverter is a buck-boost inverter, provided in one simple stage.

2.4.1 Simple Control

Figure 17 shows the traditional PWM control method as described earlier. In this case the PWM control is three phase, where V_a*, V_b*, and V_c* are the sinusoidal reference signals. The sinusoidal reference signals can be approximated as straight lines for a visual aid, because the frequency of the triangular carrier signal is much greater than the sinusoidal reference signals. So when looking at one cycle of the carrier signal, the sinusoidal reference signals will not change much. As previously mentioned the control signals are generated by comparing the reference signals and the carrier signal. S_{ap}, the control signal for the positive (upper) switch in phase leg a, for instance, is logic-high whenever V_a* is greater than the carrier signal, and logic-low whenever it is less. S_{an}, the control signal for the negative (lower) switch in phase leg a, is simply the inversion of S_{ap}. The control signals for the other phase legs are generated in the same manner.

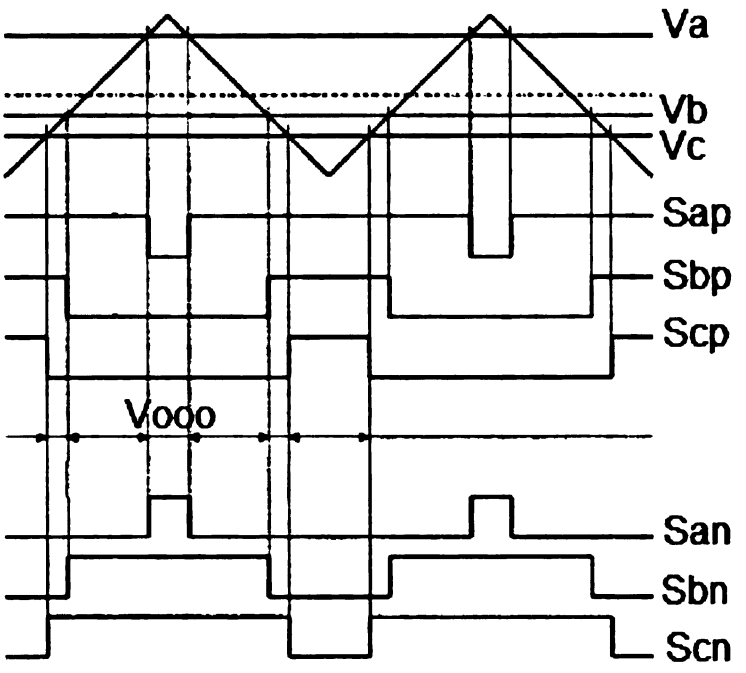

Figure 17. Traditional PWM control method

When the dc voltage is high enough to generate the desired ac voltage, the traditional PWM of figure 17 is used. When the dc voltage is not enough to generate a desired output voltage, a modified PWM with shoot through zero states will be used to boost voltage [9], as shown in figure 18. The shoot through is introduced into the zero state because this will not change the function of the PWM. As shown in figure 17, the zero state (Labeled as V_{000}) is when all of the upper (or lower) switches are gated off simultaneously creating zero voltage across the load. Introducing the shoot through here will obviously also create zero voltage across the load, therefore the shoot through does not change the operation of the PWM. As can be seen in figure 18, the shoot through zero states (highlighted grey) are evenly allocated into each phase. The shoot through is created by turning on both switches in any phase leg, for example the grey areas where both control signals S_{ap}, and S_{an} are both logic-high.

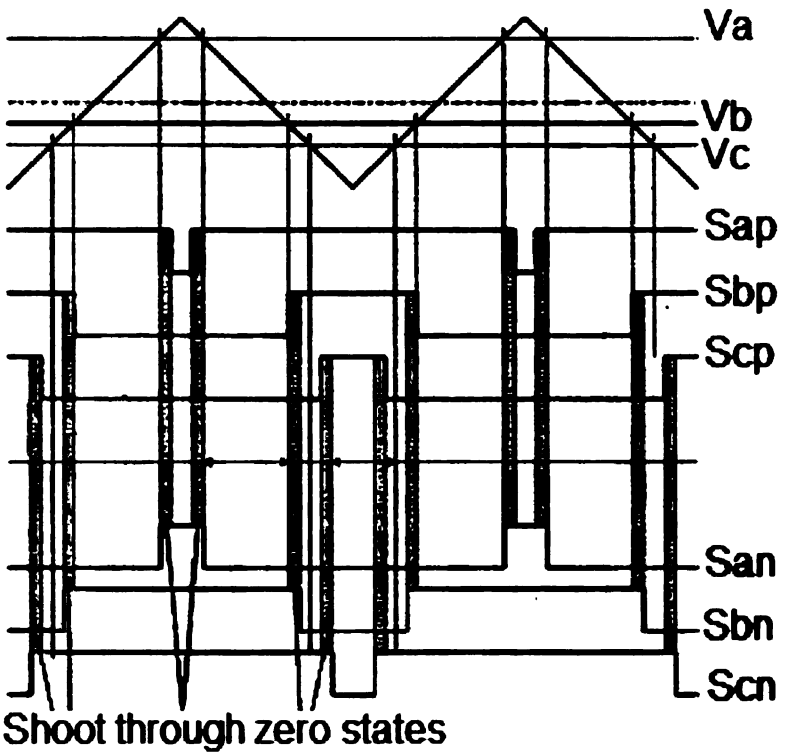

Figure 18. Modified PWM with shoot through zero states [9]

For this simple boost control, the obtainable shoot-through duty ratio decreases with the increase of the modulation index (M). The maximum shoot-through duty ratio of the simple boost control is limited to (1-M) [16], thus reaching zero at a modulation index of one. The thick curve in figure 19 shows the maximum obtainable voltage gain, MB (where B is the boost factor) versus M, which indicates no voltage boost and no voltage gain at M=1. The area left of the curve is the possible operation region under the simple control. In order to produce an output voltage that requires a high voltage gain, a small modulation index has to be used. However, small modulation indices result in greater voltage stress on the devices. Using this control method, the voltage stress across the switches is quite high, which will restrict the obtainable voltage gain because of the limitation of device voltage rating.

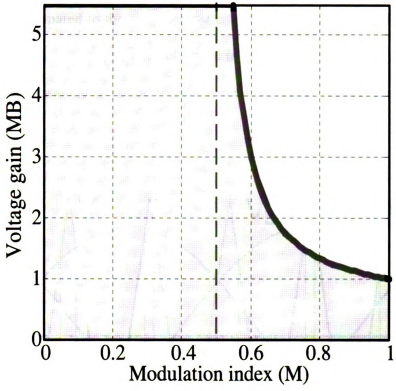

Figure 19. Voltage gain of the simple boost control [16]

2.4.2 Maximum Boost Control

Maximum boost control [16] is a control method used to produce the maximum voltage boost (or voltage gain) under a given modulation index. Reducing the voltage stress under a desired voltage gain is important to the control of Zsource inverter. Figure 20, shows the maximum boost control strategy. It is quite similar to the traditional PWM control method as described for the voltage source inverter. This control method maintains the six active states unchanged, and turns all zero states into shoot-through zero states. Thus maximum shoot through duty cycle and boost factor (B) are obtained for any given modulation index (M) without distorting the output waveform. As can be seen from figure 20, the shoot through state is obtained when the triangular carrier wave is either

greater than the maximum curve of the references (V_a, V_b, V_c), or less than the minimum of the references. Compared to the simple boost control, the possible operation region of this control method is much wider, as can be seen in figure 21, and for any given voltage gain, a higher modulation index can be used, which means lower voltage stress across the switches.

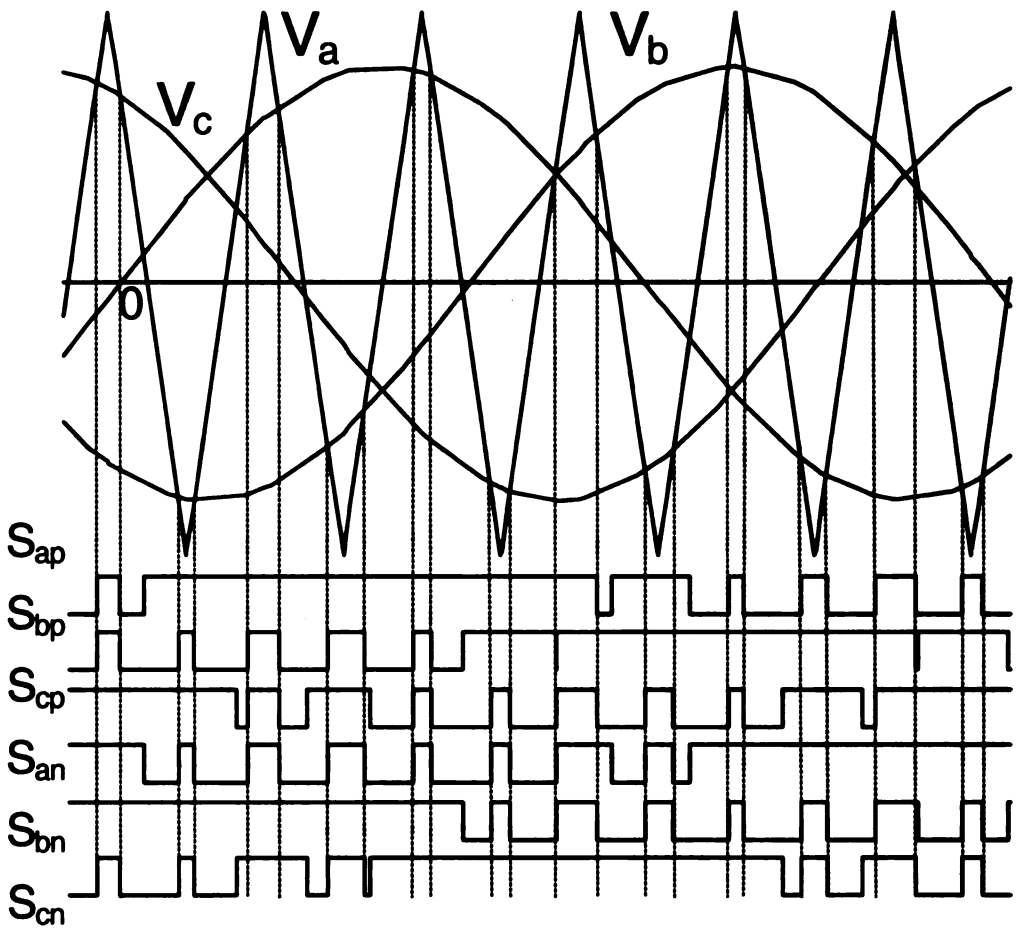

Figure 20. Maximum boost control strategy [16]

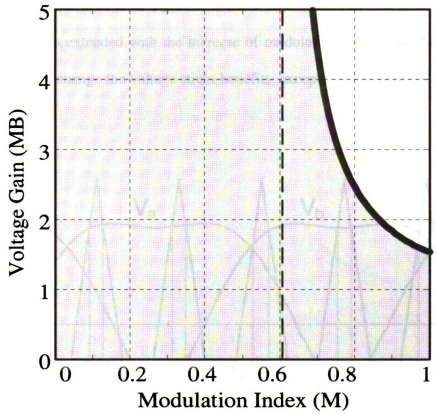

Figure 21. Voltage gain of the maximum boost control strategy [16]

As previously mentioned third harmonic injection can be used in a three-phase inverter system to increase the modulation index range. This can also be used here to increase the range of M so as to increase system voltage gain range. The control scheme is shown in figure 22. The operation principle is identical to the previous case, the only difference is that the modulation waveform is changed due to the third harmonics. In this control, the maximum modulation index $M=\frac{2}{\sqrt{3}}$ can be achieved at 1/6 third harmonic injection [15]. That is, the amplitude of the third harmonics injected is 1/6 of the amplitude of the reference signals (V_a, V_b, V_c). The voltage gain is identical to the previous control method for the same modulation index. The curve of voltage gain versus

modulation index is shown in figure 23, from which we can see that the possible operation region is extended with the increase of modulation index. The third harmonic injection does not change the voltage stress benefits, except that the range of voltage gain is extended.

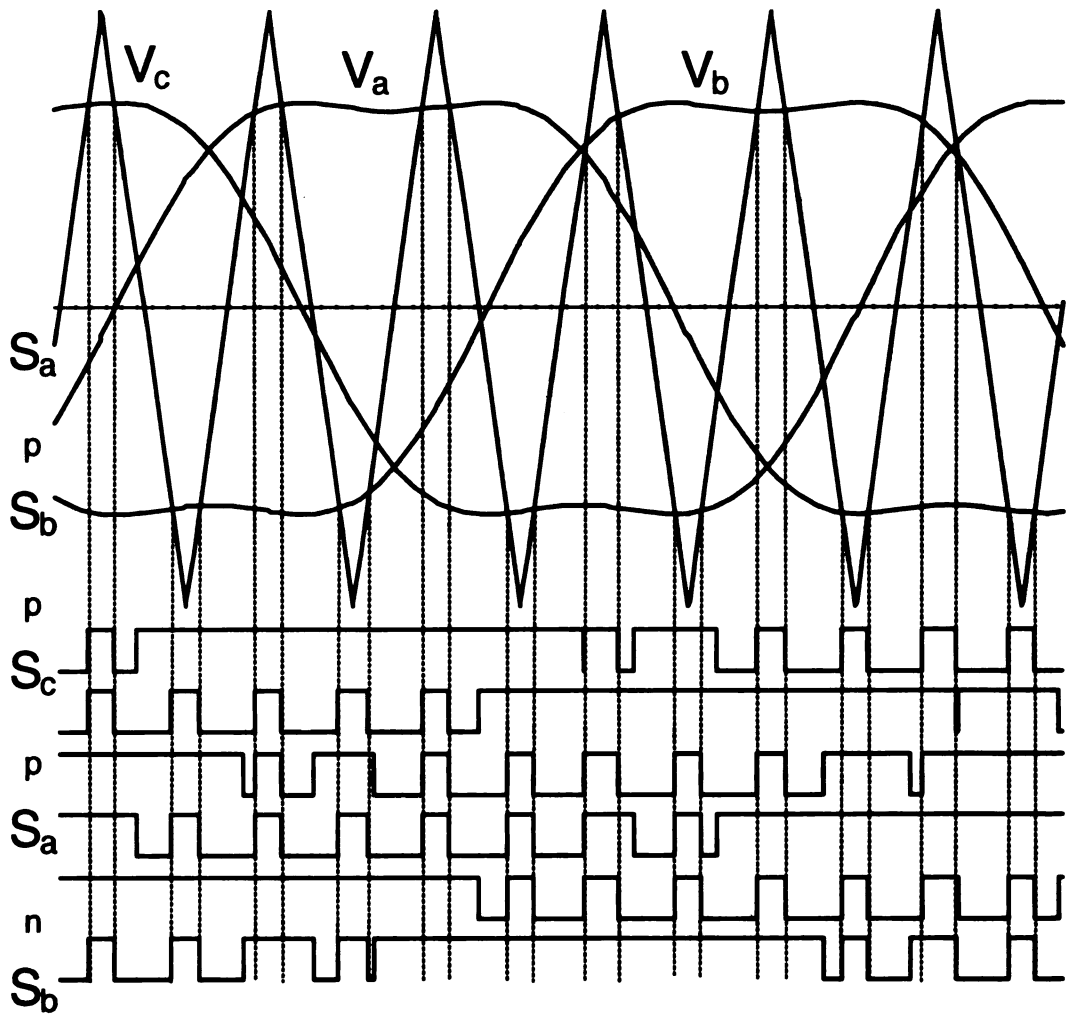

Figure 22. Maximum boost control with third harmonic injection strategy [16]

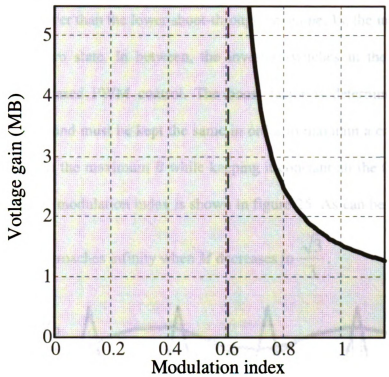

Figure 23. Voltage gain of the maximum boost control with third harmonic injection [16]

2.4.3 Maximum Constant Boost Control

The maximum constant boost control method [17] is used to achieve maximum voltage boost/gain while maintaining a constant boost viewed from the Z-source network and producing no low-frequency ripple associated with the output frequency. This maximum constant boost control can greatly reduce the L and C requirements of the Z-network. Figure 24, shows the control scheme of the maximum constant boost control method, which achieves the maximum voltage gain while always keeping the shoot-through duty ratio constant. There are five modulation curves in this control method: three reference signals, V_a, V_b, and V_c, and two shoot-through envelope signals, V_p and V_n. The upper and lower envelope curves are periodical and are three times the output

frequency. When the carrier triangle wave is greater than the upper shoot-through envelope, V_p, or lower than the lower shoot-through envelope, V_n, the inverter is turned to a shoot-through zero state. In between, the inverter switches in the same way as in traditional carrier-based PWM control. The boost factor is determined by the shoot-though duty cycle, and must be kept the same in order to maintain a constant boost. The basic point is to get the maximum B while keeping it constant all the time. The curve of voltage gain versus modulation index is shown in figure 25. As can be seen in figure 25, the voltage gain approaches infinity when M decreases to $\frac{\sqrt{3}}{3}$.

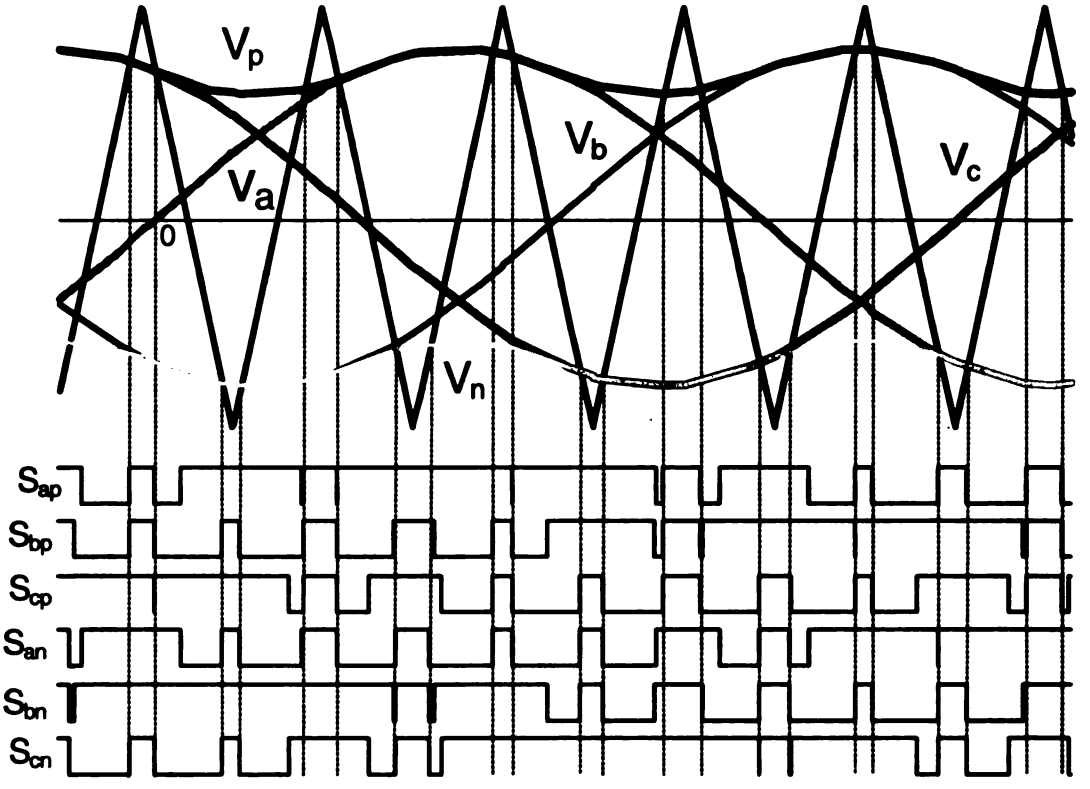

Figure 24. Maximum constant boost control strategy [17]

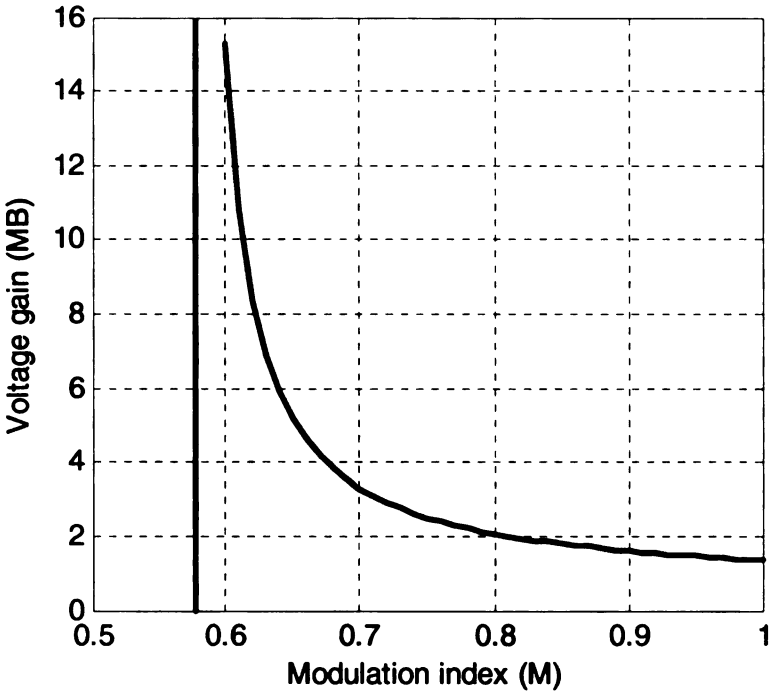

Figure 25. Voltage gain of the maximum constant boost control strategy [17]

The shoot-through duty cycle is constant and can be expressed as

$$\frac{T_0}{T} = 1 - \frac{\sqrt{3}M}{2}$$

where T_0 is the time during shoot through, T is the time while not in the shoot through state, and M is the modulation index.

The boost factor *B* and the voltage gain can be calculated:

$$B = \frac{1}{1 - 2\frac{T_0}{T}} = \frac{1}{\sqrt{3}M - 1}$$

$$\frac{\hat{V}_{ac}}{V_0/2} = MB = \frac{M}{\sqrt{3}M - 1}$$

where $\hat{v}_{ac}$ is the output ac voltage, and V_0 is the input dc voltage.

This maximum constant boost control can be implemented using third harmonic injection. A control scheme of the third harmonic injection control method, with 1/6 of the third harmonic [15], is shown in figure 26. Using the third harmonic injection a unique feature can be obtained, only two straight lines, *Vp* and *Vn*, are needed to control the shoot through time with 1/6 (16%) of the third harmonic injected. The voltage gain versus M is shown in figure 27. The voltage gain can be varied from infinity to zero smoothly by increasing M from $\frac{\sqrt{3}}{3}$ to $\frac{2}{\sqrt{3}}$ with shoot-through states (solid curve in figure 27) and then decreasing M to zero without shoot-through states (dotted curve in figure 27). The same equations from maximum constant boost with out third harmonic injection apply, that is for shoot through duty cycle, boost factor, and the voltage gain.

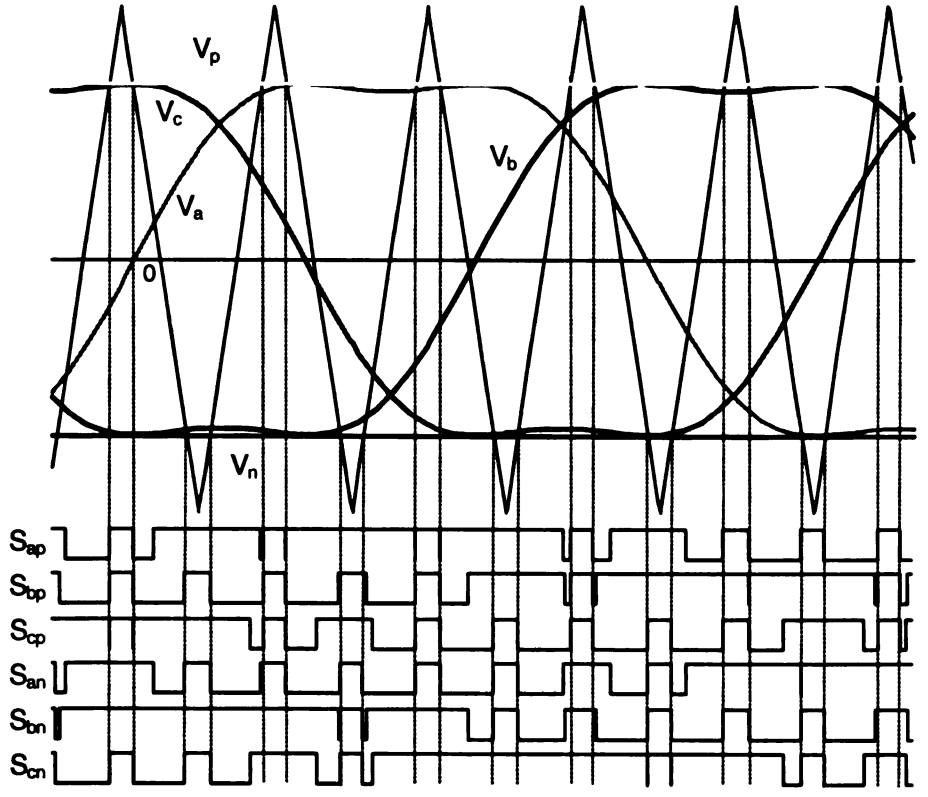

Figure 26. Maximum constant boost control with third harmonic injection strategy [17]

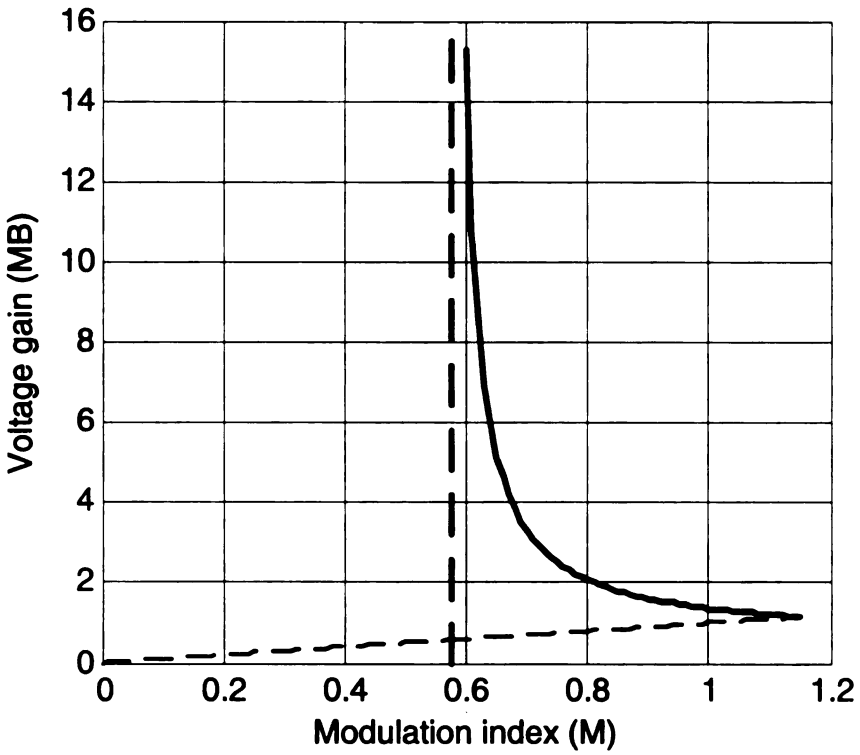

Figure 27. Voltage gain of the maximum constant boost control with third harmonic injection [17]

The voltage stresses across the devices with the three different control methods discussed are shown in figure 28. As can be seen from figure 28, the maximum constant boost control method will cause a slightly higher voltage stress across the devices than the maximum boost control method, but a much lower voltage stress than the simple control method. However, since the maximum constant boost control method eliminates line frequency related ripple, the passive components in the Z-network will be smaller, which will be advantageous in many applications such as a FCV [17]. Thus the control method used in this study will be the maximum constant boost control method with third harmonic injection.

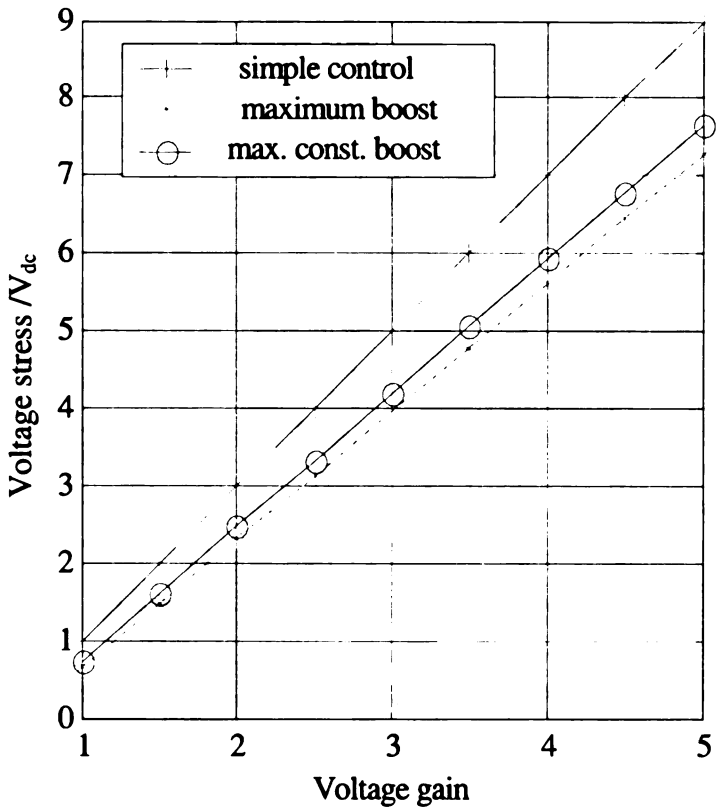

Figure 28. Voltage stress comparison of different control methods [17]

2.5 Zsource Inverter Circuit Analysis

As described in [9]. The peak dc-link voltage across the inverter bridge, $\hat{v}_i$, is expressed as

$$\hat{v}_i = B * V_0 .$$

Where V_0 is the dc source voltage, and B is the boost factor resulting from the shoot through zero state. B can be expressed from the following,

$$B = \frac{1}{1 - 2\frac{T_0}{T}} \geq 1 .$$

Given that the inverter bridge is in the shoot-through zero state for an interval of T_0, during a switching cycle with an interval T.

The peak dc-link voltage is the equivalent dc-link voltage of the inverter. On the other side, the output peak phase voltage, $\hat{v}_{ac}$, from the inverter can be expressed as,

$$\hat{v}_{ac} = M * \frac{\hat{v}_i}{2} = M * B * \frac{V_0}{2}.$$

Where M is the modulation index. This equation shows that the output voltage can be stepped up and down by choosing an appropriate buck–boost factor, B_B.

$$B_B = M * B = (0 \sim \infty).$$

The buck–boost factor B_B is determined by the modulation index M and boost factor B. The boost factor B can be controlled by the duty cycle (i.e., interval ratio) of the shoot-through zero state over the nonshoot-through states of the inverter PWM.

The capacitor voltage can be expressed as,

$$V_{C1} = V_{C2} = V_C = \frac{1 - \frac{T_0}{T}}{1 - 2\frac{T_0}{T}} V_0.$$

3. COMPARISON OF TRADITIONAL INVERTERS AND Z-SOURCE INVERTER FOR FUEL CELL VEHICLES

Three different inverter system configurations are to be investigated: the conventional PWM inverter, the dc/dc boost + PWM inverter, and the Z-source inverter. Their system configurations for fuel cell applications are shown in Figures 29, 30, and 31, respectively.

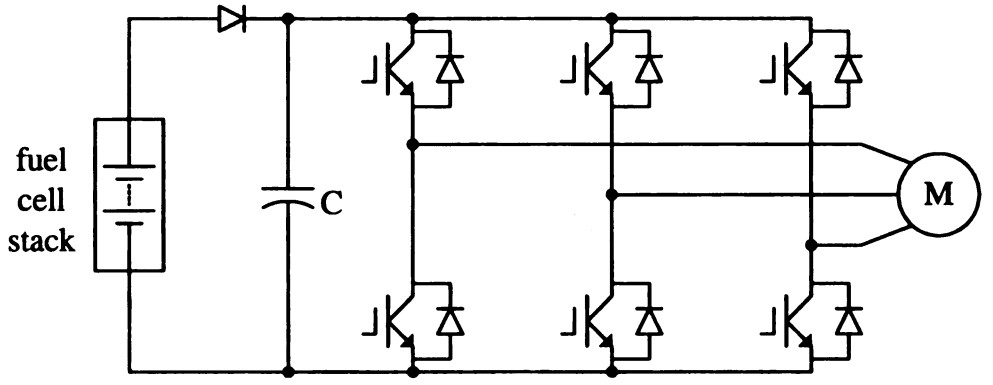

Figure 29. System configuration using conventional PWM inverter [18]

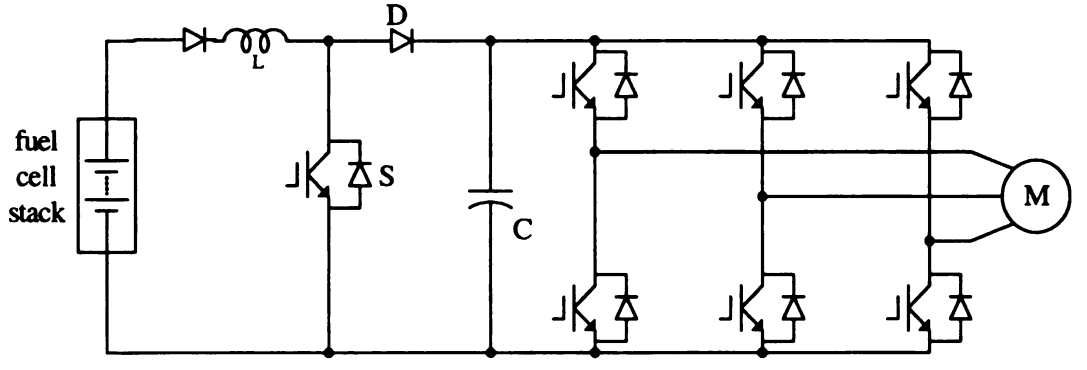

Figure 30. System configuration using dc/dc boost + PWM inverter [18]

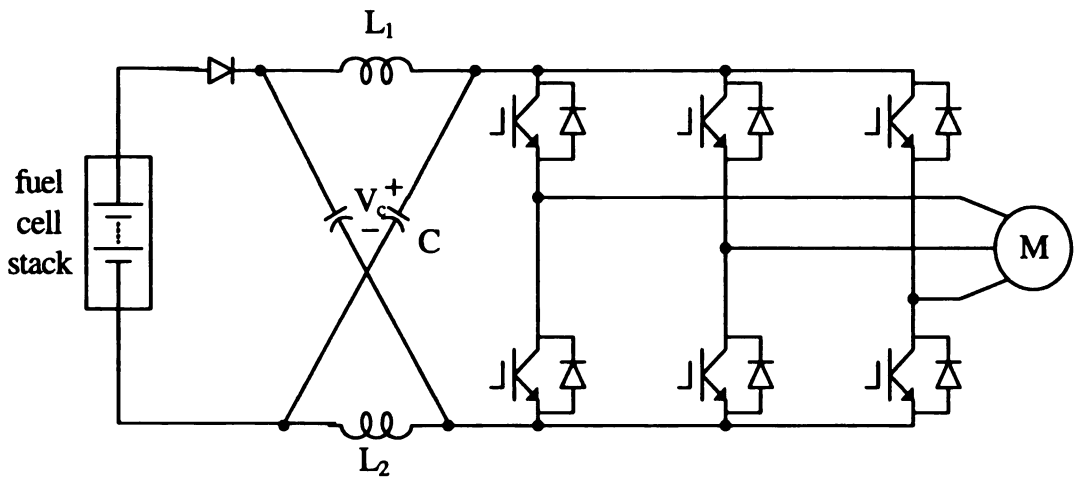

Figure 31. System configuration using the Z-source inverter [18]

3.1 Switching Device Power Comparison

In an inverter system, each switching device has to be selected according to the maximum voltage impressed and the peak and average current going through it. To quantify the voltage and current stress (or requirement) of an inverter system, Switching Device Power (SDP) is used. The SDP of a switching device/cell is expressed as the product of voltage stress and current stress. The total SDP of an inverter system is defined as the aggregate of SDP of all the switching devices used in the circuit [18]. Total SDP is a measure of the total semiconductor device requirement, thus an important cost indicator of an inverter system.

A comparison example for a 50kW fuel cell model shown in figure 32 with the following specifications is conducted in [18]. The results are given in table 1.

- Fuel cell output voltage at maximum power: 250 V;
- Maximum fuel cell output voltage: 420 V;
- Maximum power: 50 kW;
- Motor power factor at maximum power: 0.9;
- Output voltage of the boost converter: 420 V;
- Modulation index of conventional PWM inverter and dc/dc boost + PWM inverter is 1;
- Modulation index of Z source inverter is 0.9 at maximum output power. (To keep the voltage stress of the switches lower than 450 V)

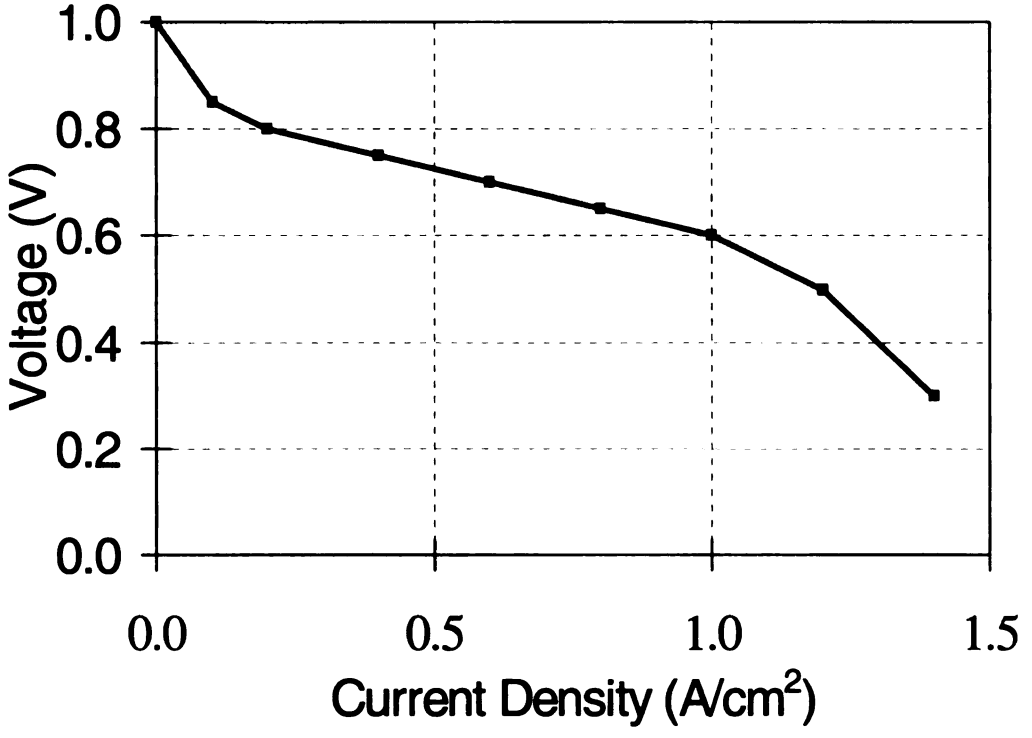

Figure 32. Typical fuel cell polarization curve [18]

Inverter Systems	Total Average SDP (kVA)	Total Peak SDP (kVA)
PWM inverter	238	747
PWM plus boost dc/dc	225	528
Z source inverter	199	605

Table 1. Switching device power comparison example [18]

The Z-source inverter's average SDP is the smallest among the three while the conventional PWM inverter's SDPs are the highest in both average and peak values. The average SDP also indicates thermal requirements and conversion efficiency.

3.2 Passive Component Comparison

From [18], an example of required passive components at input power of 50 kW is shown in Table 2 based on Current ripple through inductors <10% of average current, and the same system specification as in the SDP calculations above, at switching frequency of 10kHz:

Inverter Systems	Number of inductors	Inductance (μH)	Average inductor current (A)	Number of capacitors	Capacitor rms ripple current (A)	Capacitor voltage rating (V)
conventional PWM inverter	0	N/A	N/A	1	106	420
dc/dc boost + PWM	1	510	200	1	124	420
Z - source inverter	2	384	200	2	115	420

Table 2. Required passive components [18]

3.3 Efficiency Comparison

Efficiency is an important criterion for any power converter. High efficiency can reduce thermal requirements and cost. A comparison example is conducted in [18], with the fuel cell and motor parameters shown in Table 3. The fuel cell model is the one shown in Figure 32, with I_{pu} (per unit) =200 A, and V_{pu} (per unit)=420 V. The operation principle of the inverters are: the conventional inverter is always operating at modulation index of 1, the dc-dc boost PWM inverter boosts the dc voltage to 420 V, and the Z source inverter outputs the maximum obtainable voltage while keeping the switch voltage under 450V. The motor loss is simply modeled as the loss at the stator resistor. The same motor model is used to calculate the motor loss. The selected devices for loss calculation are: The switches for the main inverters are FUJI IPM 6MBP300RA060, the switch for the dc/dc boost converter is FUJI 2MBI 300N-060.

Only the semiconductor devices loss is considered. The calculation results are also shown Figures 33, and 34 respectively.

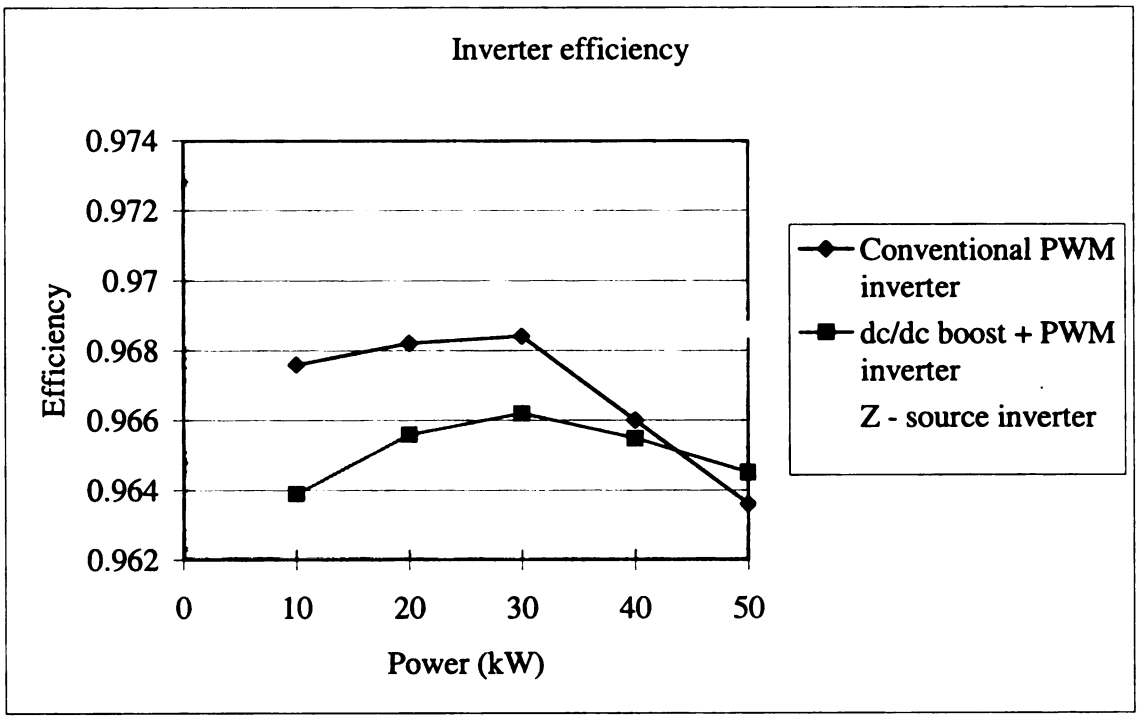

Figure 33. Calculated efficiency of inverters [18]

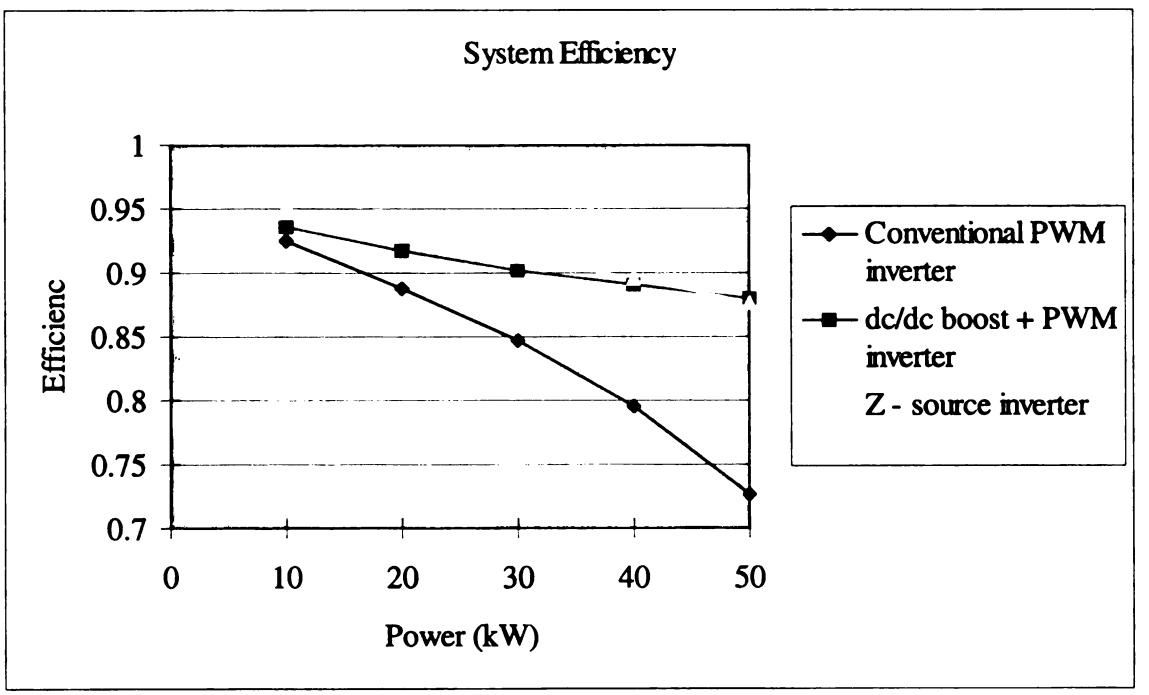

Figure 34. Calculated efficiency of inverters plus motor [18]

From the above comparisons, the Z source inverter provides the highest efficiency.

Power Rating		50 kW 56 kVA	40kW 47kVA	30 kW 38 kVA	20 kW 27 kVA	10 kW 14 kVA
Fuel cell voltage (V)		250	280	305	325	340
Motor current (A)	Conventional PWM inverter	209.4	158.5	115.9	77.3	39.7
	Dc/dc boost +PWM inverter	124.7	105.6	84.2	59.9	32.1
	Z – source inverter	129.5	105.3	81.1	56.2	29.6

Table 3. Operation Conditions at Different Power [18]

3.4 CPSR Comparison

Constant power speed ratio (CPSR), the ratio between the top speed of a motor and its base speed, is limited mainly by available dc voltage of the PWM inverter. The fuel cell voltage decreases as the current drawn increases, which greatly limits the motor's power output and efficiency at high speed. For the conventional PWM inverter with the fuel cell model described above, the fuel cell voltage is the dc voltage of the inverter, which drops to 250 V at 200 A. From the 250 V dc, the conventional PWM inverter can only yield 170 V to the motor. This low motor voltage limits CPSR and lowers mechanical output power and efficiency. Both the PWM inverter with dc-dc boost and Z-source inverter can keep the inverter dc voltage constant at or above 420 V, which in turn increases CPSR by a factor of 1.68 [18]. In other words, the motor voltage

produced by these inverters is 1.68 times that produced by the conventional PWM inverter, thus the same motor can output 1.68 times the power than when driven by the conventional PWM inverter.

3.5 Comparison of Traditional Inverters and Z-Source Inverter for Fuel Cell – Battery Hybrid Vehicles

As previously mentioned the Z-source inverter has two independent control freedoms. The following analysis is provided to show that the shoot-through duty cycle D_0, can be used to control the battery terminal voltage Vb (thus controlling SOC), and the D_0 and the modulation index M can be used to control the output ac voltage to the motor $\hat{v}_{ac}$. From [9], we have

$$V_b = V_c = \frac{1-D_0}{1-2D_0} V_0 \quad \text{and,} \quad \frac{\hat{V}_{ac}}{V_0/2} = M \frac{1}{1-2D_0},$$

where Vb equals capacitor voltage Vc, and V_0 is the fuel cell voltage. The above equations show that we can independently produce any desired output ac voltage (limited by the voltage ratings), control the battery terminal voltage (i.e. SOC), and control the fuel cell voltage (or power), by controlling the shoot-through duty cycle, and modulation index. The FC HEV uses a battery to assist the fuel cell system output the requested power to the traction motor, capture excess power from the fuel cell, and to absorb energy from regenerative braking. The FC HEV using the conventional inverter, Figure 35, must use a bi-directional dc-dc converter to control the SOC of the battery, because the modulation index is the inverters only control freedom. Also, the conventional inverter is a buck (step-down) inverter, the output ac voltage is limited below the fuel cell

voltage. Because of the wide voltage range of the fuel cell, the conventional inverter imposes high stresses to the switching devices.

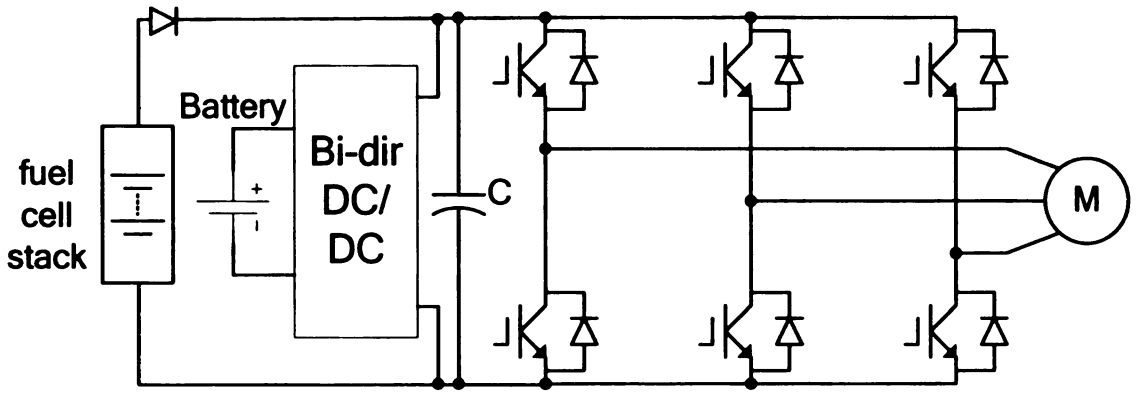

Figure 35. System configuration using a conventional inverter

The dc-dc boosted inverter, Figure 36, can improve these stresses, at the price of higher cost and complexity. The dc-dc boost converter is used to boost (step-up) the voltage from the fuel cell, to a steady dc bus voltage, and the inverters output ac voltage is controlled by the modulation index. The system configuration using the dc-dc boosted inverter typically uses a bi-directional dc-dc converter to control the SOC of the battery [19].

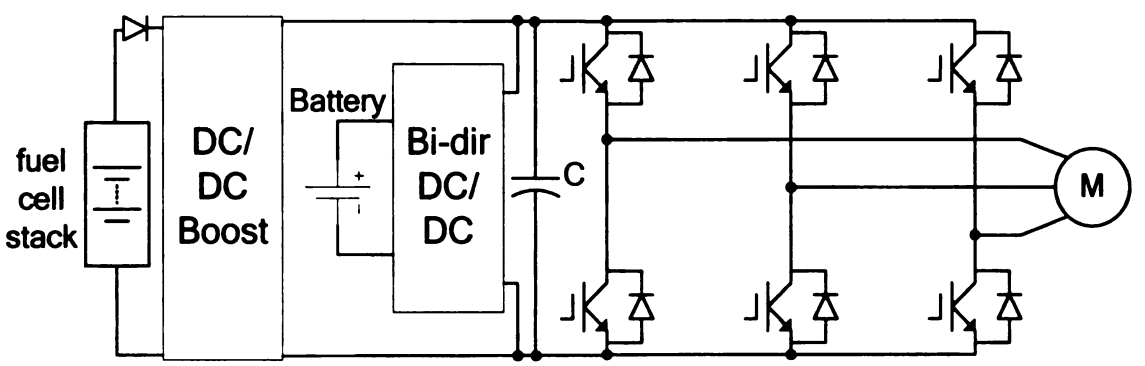

Figure 36. System configuration using a DC-DC boosted inverter

By using the Z-source inverter system configuration, Figure 37, we eliminate the dc-dc converters. This can be achieved because the Z-source inverter has two independent control freedoms. By controlling the shoot-through duty cycle we can control the battery SOC, and by controlling the modulation index we can control the output ac voltage. This advantage of the Z-source inverter will result in a much more cost efficient, and power efficient hybrid FCV.

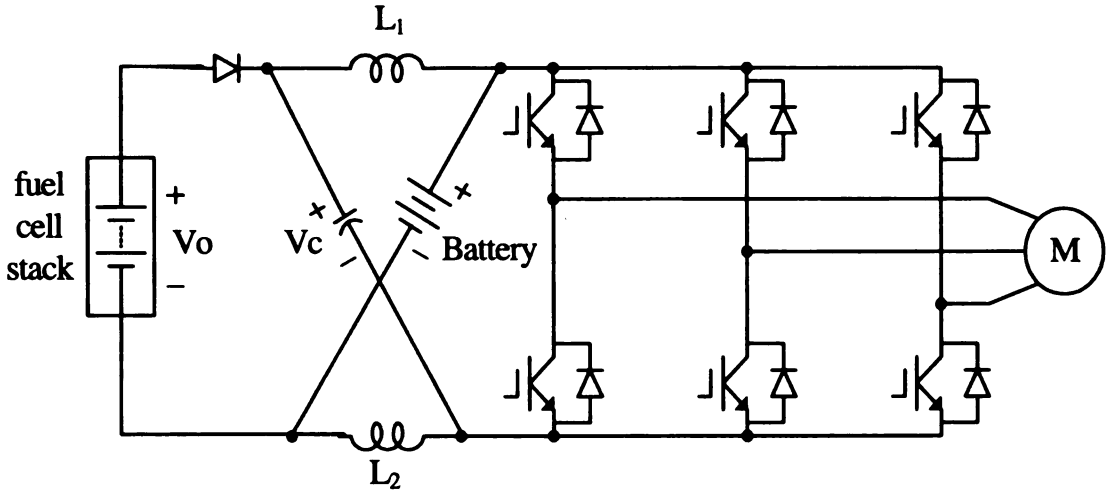

Figure 37. System configuration using a Z-source inverter

3.6 Comparison Conclusions

The comparison results show that the Z-source inverter can increase inverter conversion efficiency by 1% over the two existing systems and inverter-motor system efficiency by 2 to 15% over the conventional PWM inverter. The Z-source also reduces the total average SDP by 15%, which leads to cost reduction. Moreover, the constant power speed ratio is greatly (1.68 times) extended over the system driven by the conventional PWM inverter. Thus, the Z-source inverter system can minimize stresses

and size of the motor and increase output power greatly. It has also been shown that no dc-dc converters are needed to control the battery SOC. Along with these promising results, the Z-source inverter offers a simplified single stage power conversion topology and higher reliability because the shoot through can no longer destroy the inverter.

4. REVIEW OF CURRENT FUEL CELL VEHICLE TECHNOLOGY

4.1 FCV Operating Modes

As seen in figure 38, the system configuration consists of the fuel cell stack, the battery, the controller (inverter), and the traction motor. The main source of the vehicles power is the fuel cell. The secondary power source is the battery, which also stores excess energy from the fuel cell, and from regenerative braking. The four utilized operating modes are outlined in the following [20].

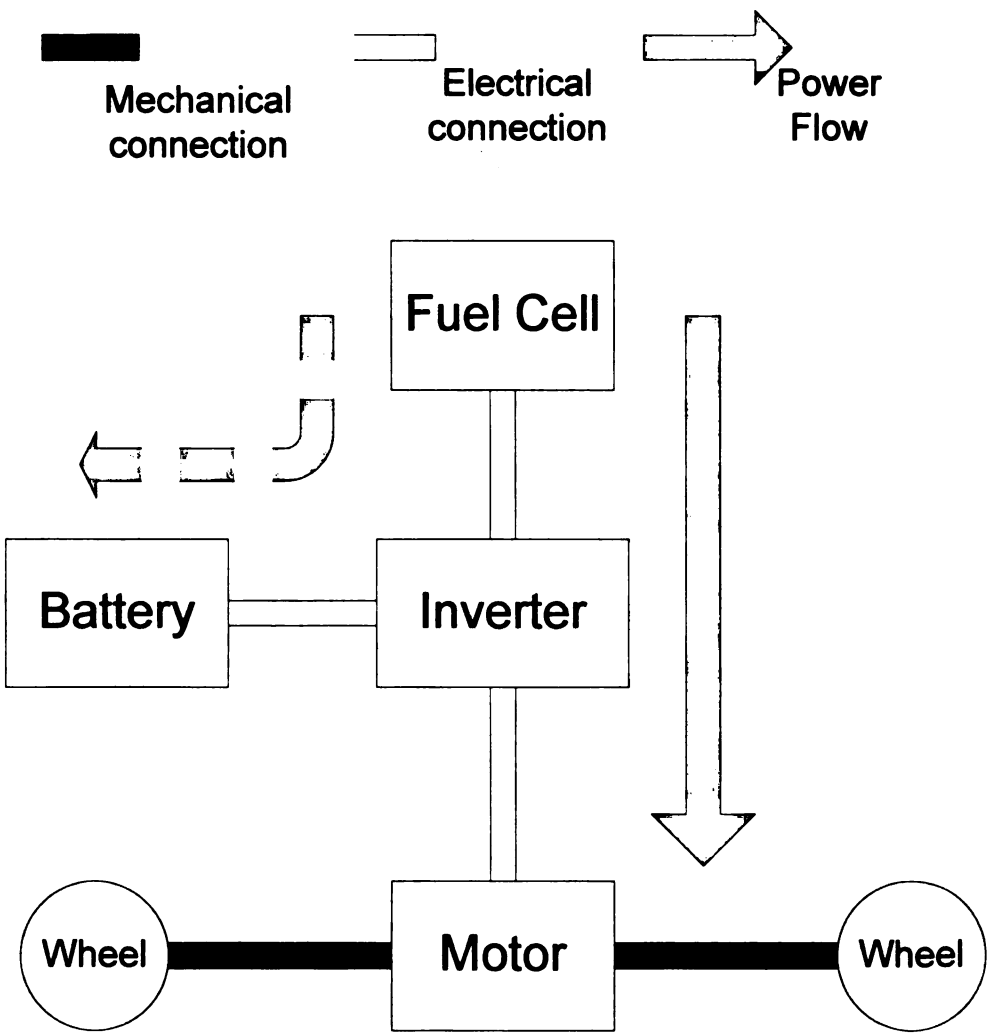

Figure 38. Medium power operating mode

4.1.1 Mode 1, medium power

The medium power operating mode, as shown in figure 38, normally occurs after the vehicle accelerates and the vehicle maintains a fairly constant speed, highway travel is an excellent example of this. While in the medium power mode, the vehicle traction motor only receives power from the fuel cell.

4.1.2 Mode 2, high power

The high power mode usually occurs during acceleration, or uphill driving. While in the high power operating mode, both the fuel cell and the secondary battery provide power to the traction motor, Figure 39. The battery can also speed up the vehicles response time for a request of acceleration, because the fuel cell typically has a slow response time.

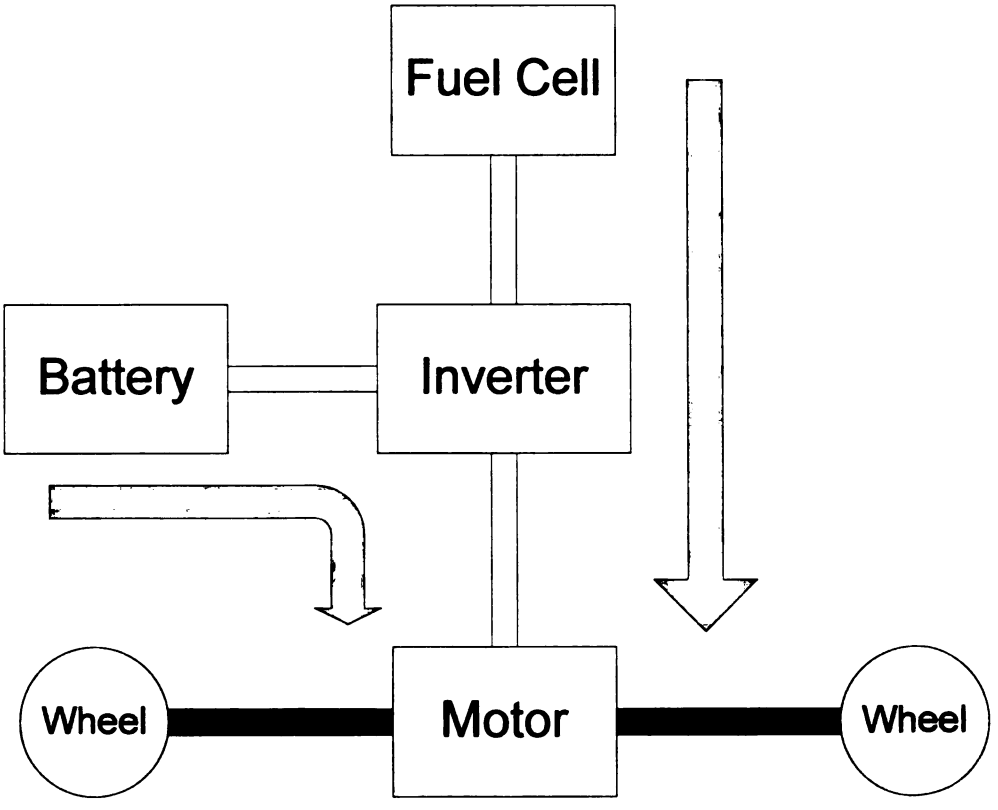

Figure 39. High power operating mode

4.1.3 Mode 3, low power

The low power operating mode, Figure 40, typically occurs at low speed, an example of this would be driving slowly in heavy traffic. Because of the parasitic loads, such as the air compressor, associated with the fuel cell, the fuel cell system efficiency decreases when operated under low power [20]. Thus the vehicle will be operated strictly as a battery powered electric vehicle under low power.

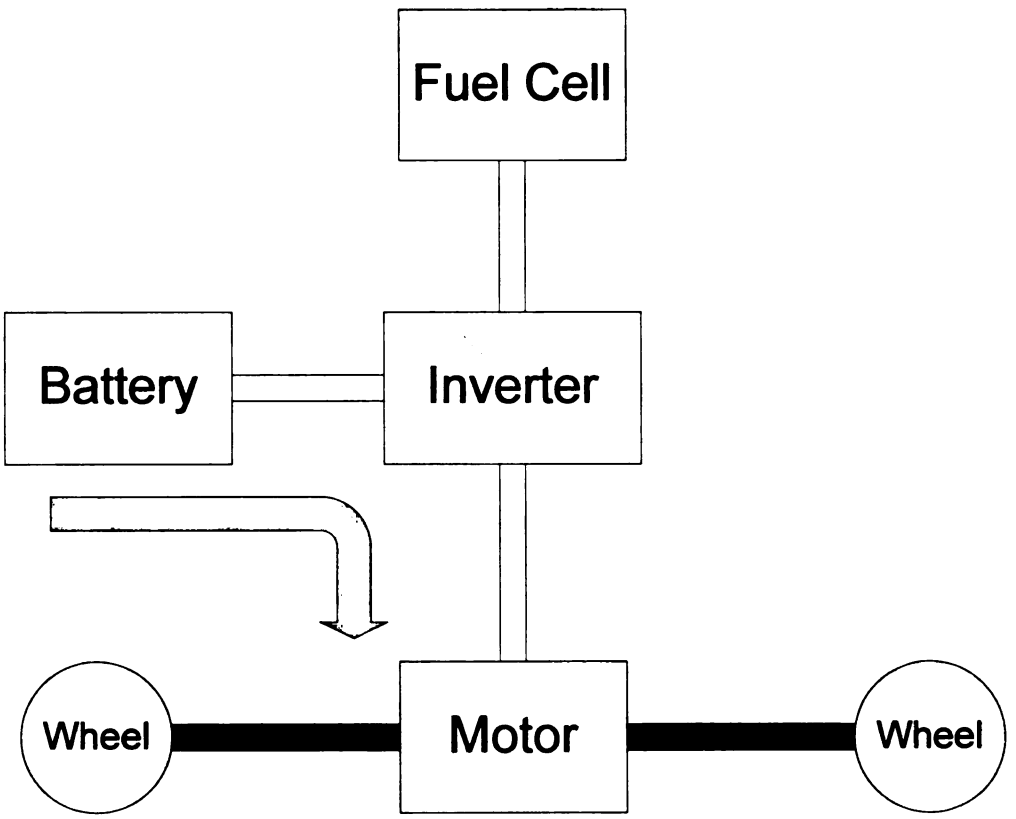

Figure 40. Low power operating mode

4.1.4 Mode 4, regenerative braking

Regenerative breaking, Figure 41, usually occurs when the vehicle operator presses the brake pedal, or when the vehicle coasts downhill. During regenerative breaking the fuel cell produces no power, and the electric motor acts like a generator,

using the wheels to apply torque to the motor to generate electrical power, this torque in turn slows the vehicle down. The energy created during regenerative braking is stored in the battery until needed. It is important to note that without shoot-through the Z-source inverter operates in the same way as traditional inverters, providing the capability for regenerative braking.

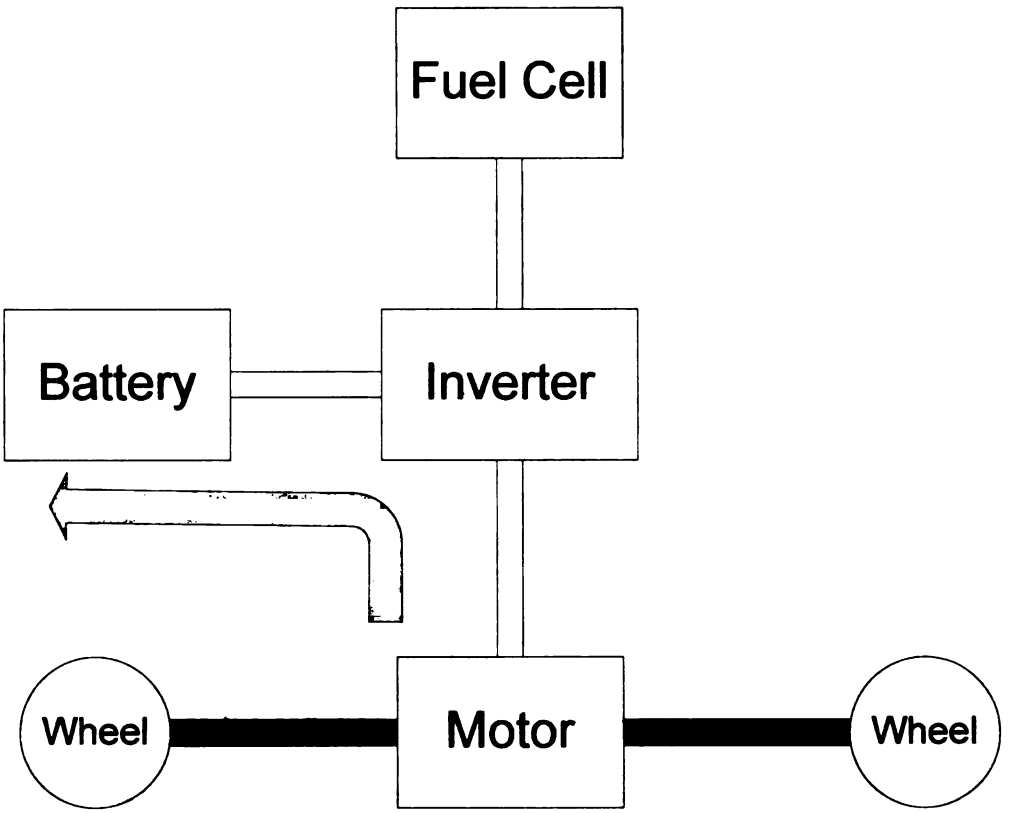

Figure 41. Regenerative braking operating mode

It is important to mention that in any of the operating modes, if the SOC of the battery becomes too low, the fuel cell power will be increased to provide power to recharge the battery [20].

4.2 Current FCV Technology

A review was conducted of work performed to date in the area of FCV design. Several companies and research institutions have performed work in the FCV area, and a summary of recent work, focusing on the power electronics, is listed in this section.

4.2.1 Texas Tech University Fuel Cell Vehicle

The Texas Tech FCV [21] is propelled by two electric motors, and powered by a combination of batteries and a fuel cell. A 1997 Chevrolet Lumina is used and expected to achieve 60 mpg and have zero emissions. The desired requirements are 0 to 60 mph in under 16 seconds, and a driving range of 325 miles. This acceleration requirement for a 4400 pound vehicle, requires a motor between 100 and 150 kW depending on the transmission. They selected to use two ac induction motors, because they are much less expensive than dc brushless motors, however the dc brushless motors are lighter and more efficient. They used 23, 38Ah 12V sealed lead acid batteries, connected in series, resulting in 276V, a high enough voltage to run the motors. Thus the inverter can be connected directly across the batteries. The maximum power created by the batteries is approximately 100kW. While the maximum power from the fuel cell is 20kW (60V @ 333A). A dc-dc converter is connected in parallel to each of the batteries, which steps down the voltage from the fuel cell to a voltage suitable for charging the batteries. The dc-dc converters have the following characteristics, input voltage range: 50V to 100V, output voltage: 12V to 15V (adjustable), input current: 15A (max), output current: 50A (max).

4.2.2 Ford Fuel Cell Vehicle

The Ford P2000 [22] is built on the contour platform, and consists of only one power source, the fuel cell, actually 3 fuel cells connected in series, producing a maximum voltage of 385V. The P2000 is the simplest example of a FCV, because no battery is incorporated. However without a battery the P2000 will not be able to benefit from regenerative braking, which could lead to a loss of up to 30% in some urban driving cycles. The P2000 uses a 67kW ac induction motor. No dc-dc boost converter is needed because the fuel cells produce high enough voltage to run the motor. Therefore the inverter is directly connected to the fuel cells. The Inverter has the following characteristics, maximum current: 280A, minimum voltage: 200V, maximum voltage 385V, and nominal voltage of 255V.

4.2.3 Jeep Fuel Cell Vehicle

In October 2000, DaimlerChrysler introduced the Jeep Commander 2 methanol FCV [23] in Lansing, Michigan. To use methanol as the fuel, the vehicle must have an on board methanol fuel reforming system to extract hydrogen from the methanol. This results in a vehicle that is no longer zero emissions, but it is still much cleaner than a conventional vehicle using an internal combustion engine. The Jeep FCV incorporates two 38kW fuel cells, operating at a voltage between 220V to 270V. Also a 28Ah, 324V (nominal) battery, capable of producing 90kW is used as a secondary power source, and connected directly to the inverter bus. A dc-dc boost converter is used to boost the fuel cell voltage to charge the batteries and drive the two 83kW induction motors more efficiently.

4.2.4 Toyota Fuel Cell Vehicle

In the Toyota FCV [20] the 90kW maximum fuel cell and the traction inverter are connected directly in series, with the 6.5Ah battery connected in parallel to the inverter bus through a 20kW dc-dc converter. The Toyota FCV uses a permanent magnet ac induction motor capable of 83kW maximum power. The battery connected in parallel to the inverter bus through a dc-dc converter is mainly used to provide power assist when the fuel cell response is delayed, or when the vehicle is driven under high loads. The battery also absorbs the energy recovered by regenerative braking, and acts as the vehicles primary power source under low loads.

5. SIMULATION

In this chapter simulations will be used to verify the Z-source inverter can be used to provide the above-mentioned hybrid system operating modes, control of battery SOC, control of fuel cell voltage (or power), and control of output voltage (or power). The simulations will be run using a software package called SABER. Saber software [25] simulates physical effects in different engineering domains (hydraulic, electric, electronic, mechanical, etc.) as well as signal-flow algorithms and software. Saber software is used in the automotive, aerospace, power and IC industry to simulate and analyze systems, sub-systems and components to reduce the need for prototypes. Many innovations in the automotive sector today are enabled by hybrid technologies where software controlled electro-mechanical components replace traditional mechanical components.

5.1 Simulation Setup

The Zsource inverter shown in figure 41 was modeled and simulated using SABER. To examine this system, first fuel cell and battery models are needed.

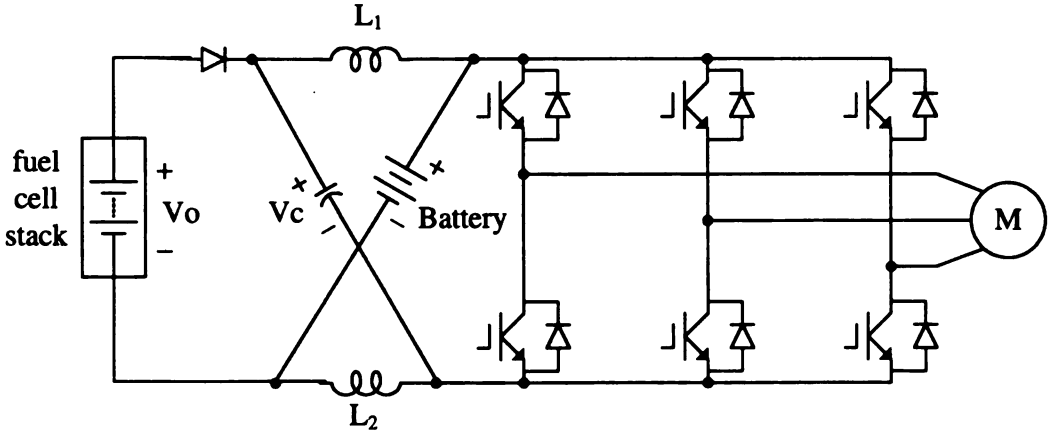

Figure 42. Schematic of simulation model

5.1.1 Fuel Cell Stack Model

Although there are many complex subsystems and parasitic loads associated with a fuel cell, when considering the power electronics, we are mainly concerned with the voltage, and current. It is possible to model a fuel cell stack in a much more fundamental manner, incorporating electrochemistry, thermal characteristics, and mass transfer, but such a model is not necessary for the analysis as accomplished in this work. The fuel cells voltage (and power) is determined by two main factors. First the rate at which hydrogen flows through the fuel cell establishes the level of the V-I polarization curve [26]. Second the amount of current drawn by the inverter determines the point on this curve where the fuel cell will operate. Thus, by controlling the amount of current drawn by the inverter, the fuel cell voltage and power can be controlled.

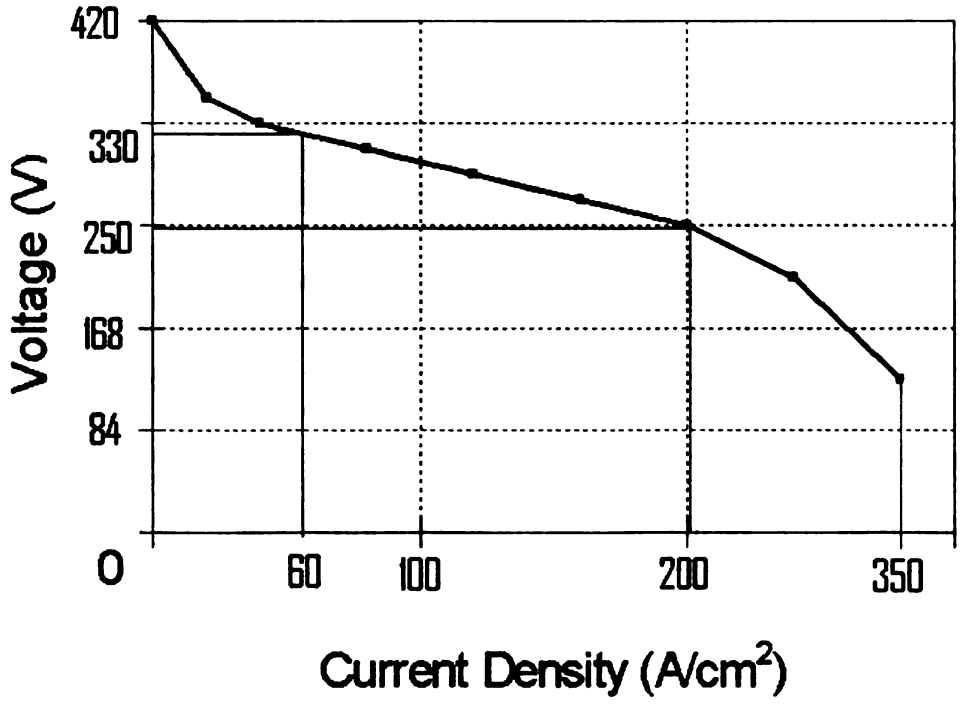

Figure 43. Fuel cell polarization curve

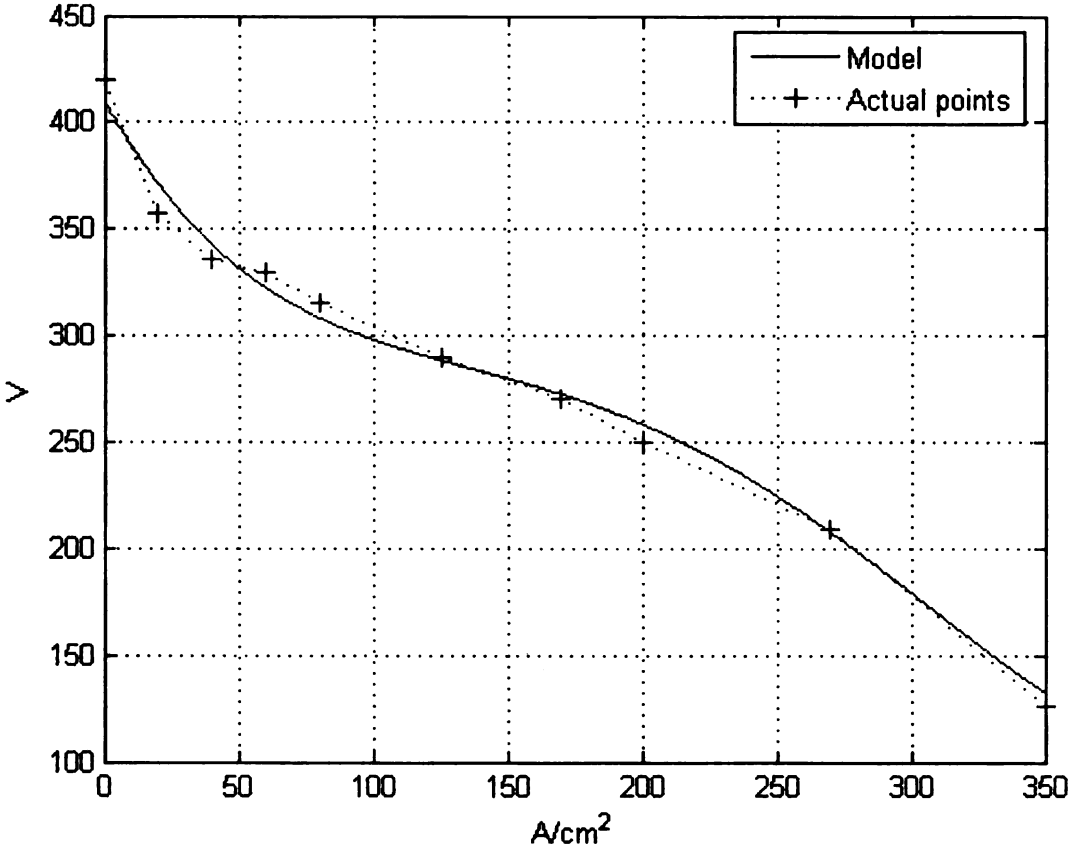

Figure 44. Comparison of fuel cell polarization curve and model equation

To create a fuel cell model, an equation is used to approximate the V-I polarization curve of Figure 43. Figure 44 shows the polarization curve of the 50 kW fuel cell stack that was used in this study, along with the model equation curve. The equation given in MATLAB, a common mathematics software program, by basic curve fitting the points on the "Typical Fuel Cell Polarization Curve" is

V= 6.4657e-008*I.^4 -5.7400e-005*I.^3 + 0.0163*I.^2 -2.2381*I +410.0976

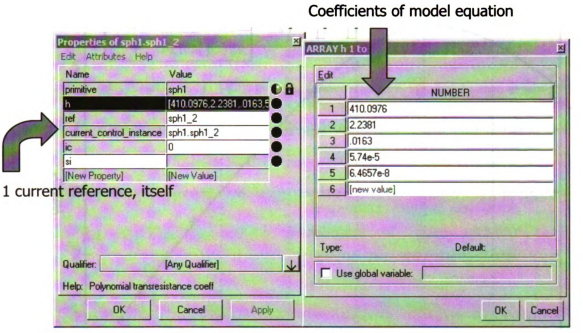

Figure 45. Properties of the fuel cell model

To create the fuel cell model in SABER, a current controlled voltage source (CCVS) was used. The coefficients of this model equation were used in the CCVS as shown in Figure 45, and the voltage of the CCVS is controlled by its own current.

To check the accuracy of the CCVS fuel cell model compared to the "Typical Fuel Cell Polarization Curve" the power versus current graph as seen in Figure 46 is checked to verify that the curves do not vary greatly. The power versus current graph does indeed verify the accuracy of the fuel cell model equation. However one point from the "Typical Fuel Cell Polarization Curve" does not line up accurately, it can be seen that when the "Typical Fuel Cell Polarization Curve" is at 50kW the fuel cell model is actually at around 53kW. All other points from the "Typical Fuel Cell Polarization Curve" line up very accurately.

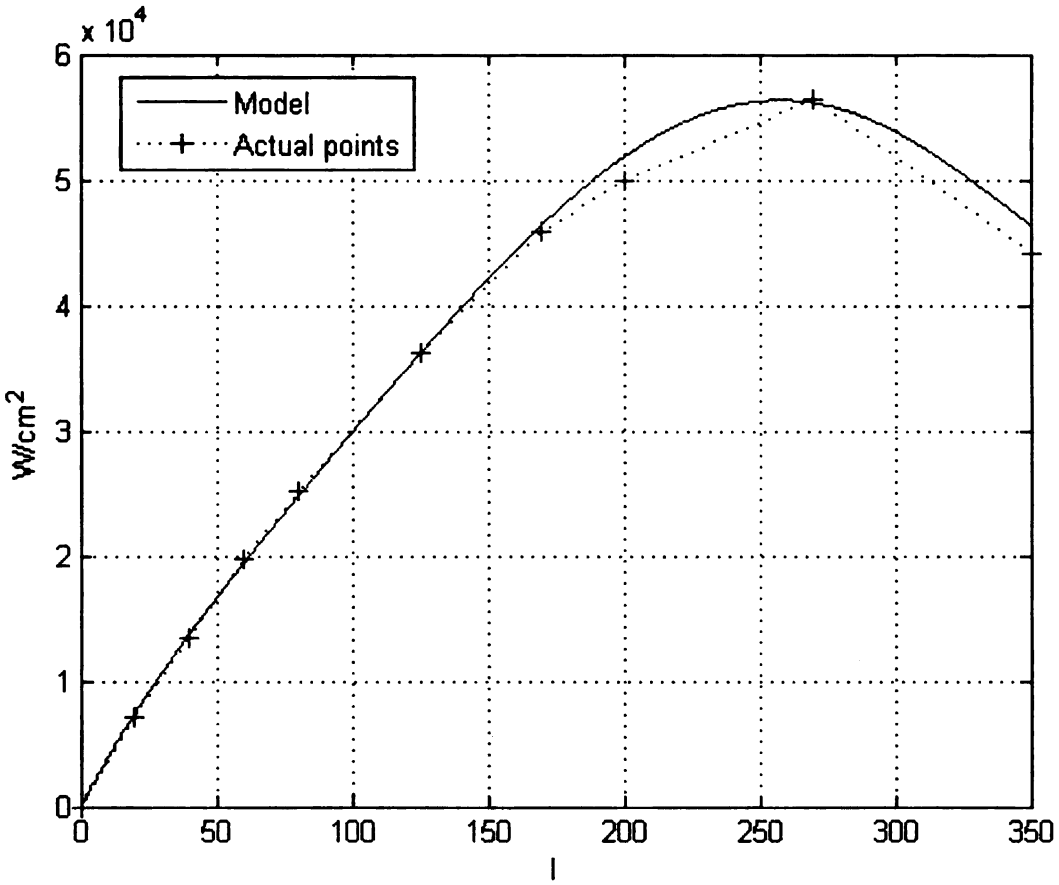

Figure 46. Fuel cell model power versus current graph comparison

5.1.2 Battery Model

FCVs employ a battery for storing energy and to handle the load dynamics. The battery is used to supply supplementary power to the motor, allowing the fuel cell to operate in an efficient and safe region [27]. Depending on the batteries SOC, it can be charged, discharged, or held constant. The SOC can be controlled two ways. First, the battery terminal voltage (i.e. SOC) is controlled by the shoot-through duty cycle. Second, the fuel cell power can be adjusted. That is, if the fuel cell power is greater than the load power the SOC increases, or if the fuel cell power is less than the load power the SOC decreases. Changes in the SOC occur due to load leveling, because the load dynamics can

change much faster than the fuel cell can respond. For example as a FCV climbs a hill the extra power needed to maintain speed comes from the battery, and as the vehicle descends the battery will absorb the extra power created by the fuel cell. SABER has a lithium-ion battery model in its MAST parts Library, which is used in this study. The properties of the lithium-ion battery model are shown in Figure 47.

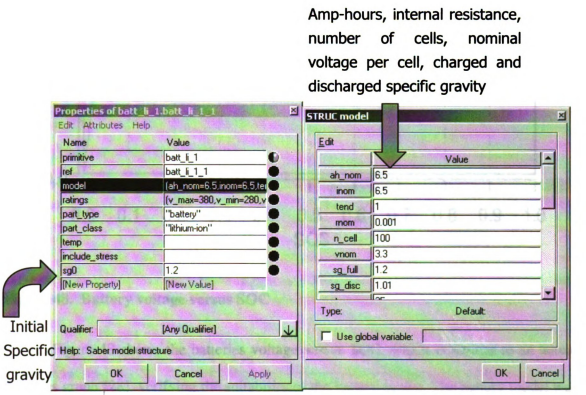

Figure 47. Properties of the lithium-ion battery model

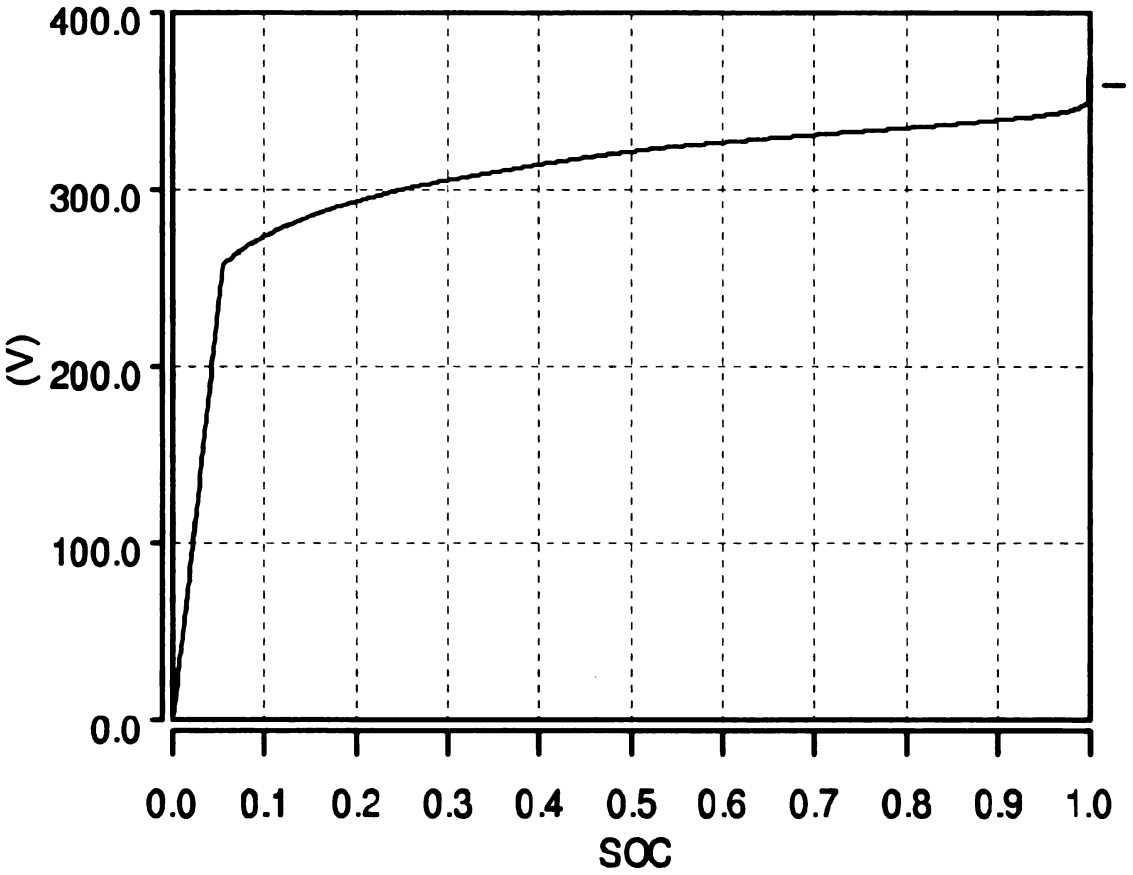

Figure 48. Battery voltage versus SOC

Figure 48 shows the batteries voltage versus SOC, which is similar to an actual batteries graph [28], verifying the suitability of the battery model. The battery model was set to 6.5 Ah, the specific gravity and number of cells was set to achieve the nominal voltage.

5.1.3 Control

As previously mentioned maximum constant boost control with third harmonic injection [17] is the control method used in this work. Figure 49 shows the control scheme of maximum constant boost control with third harmonic injection. The final

simulation schematic is shown in figure 50. The reference signals V_a, V_b, and V_c are each created with two ac voltage sources in series, the reference signal added to the 1/6 amplitude third harmonics [15]. The triangular carrier signal is created by a periodic voltage source. The upper and lower shoot through envelope voltages, V_p and V_n are each created by comparing dc voltage reference signals V_{pref} and V_{nref} along with the carried signal. The gate control signals S_{an}, S_{ap}, S_{bn}, S_{bp}, S_{cn}, and S_{cp} are created by comparing the reference signals along with the carrier signal, as in traditional PWM, and using a logic OR gate to combine that signal along with V_p and V_n. So for example S_{ap} is logic high when ever the reference signal V_a is greater than the carrier signal, OR the envelope voltage reference V_{pref} is less than the carrier signal, OR the envelope voltage reference V_{nref} is greater than the carrier signal.

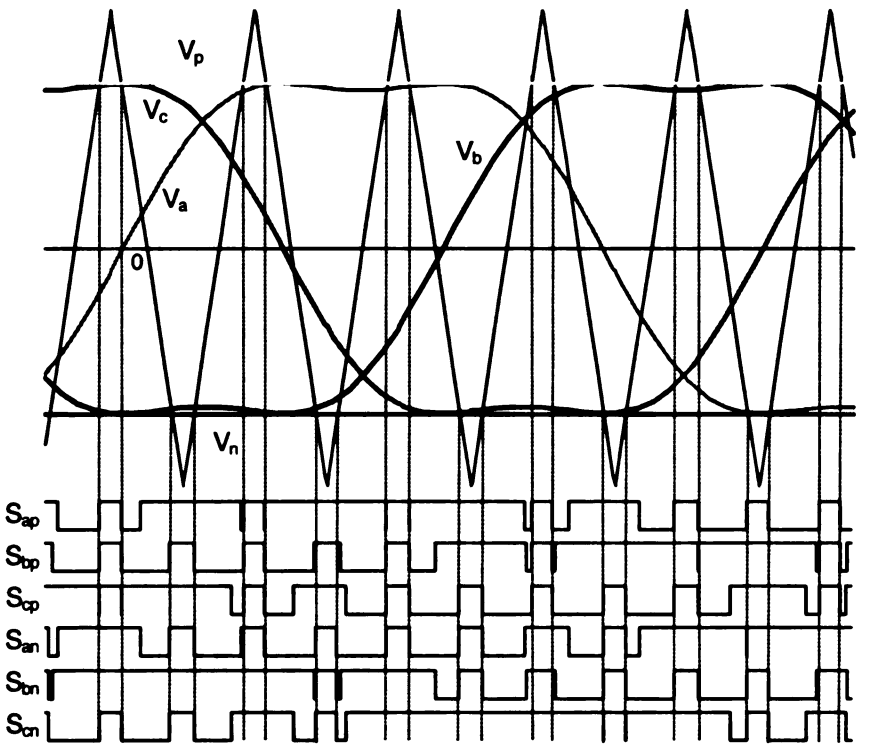

Figure 49. Maximum constant boost control with third harmonic injection [17]

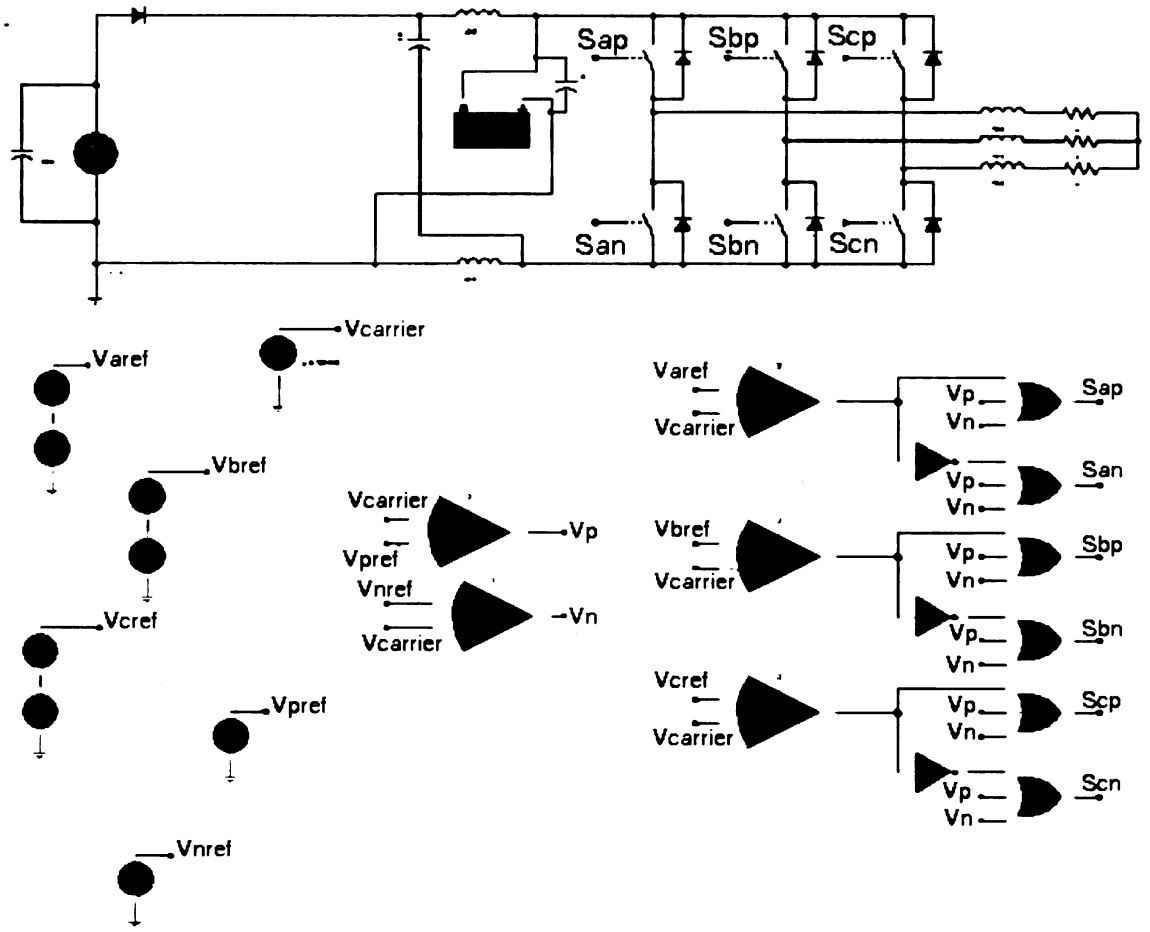

Figure 50. Final simulation schematic

5.2 Simulation

To verify the Z-source inverter can be used to provide the above-mentioned hybrid system operating modes, control of battery SOC, and control of output voltage (or power), three cases are examined and simulated. In these cases the circuit parameters are L1=L2=200μH, C1=400μF, C2 has been replaced with a 6.5Ah battery with a nominal voltage of 330V, switching frequency of 10 kHz, and using maximum constant boost

control with third harmonic injection [17].

5.2.1 Simulation Case 1

The fuel cell voltage is kept constant at 300V (P=30kW), and the load power is varied from 30kW, to 55kW, to 5kW, back to 30kW. As one would expect the battery SOC should remain constant while the load is at 30kW (Pin=Pout). When the load is increased to 55kW (Pin<Pout) the battery should supply the additional power requested by the load, thus the SOC will decrease. When the load is decreased to 5kW (Pin>Pout) the additional power provided by the fuel cell will charge the battery, increasing the SOC.

These results are verified by simulation, Figure 51, starting from the top, the fuel cell voltage is constant, and the fuel cell current is fairly constant. Next are the battery voltage, SOC, load voltage, load current, and load power. Initially the load absorbs 30kW, and the SOC stays constant. The load is then increased to 55kW and the SOC decreases. Next the load is decreased to 5kW, and the SOC increases. Finally the load is returned to 30kW and the SOC remains constant.

This simulation shows that we can operate the fuel cell at an efficient operating point, while the battery handles the load dynamics. This also verifies the Z-source inverter can be used to provide the medium, and high power operating modes. Whilst the load is increased to 55kW the battery and fuel cell both provide power to the load, verifying the high power mode. The medium power mode is verified when the load is consuming 30kW, the fuel cell provides power to the load, and while the load is at 5kW, the fuel cell provides power to the load and charges the battery.

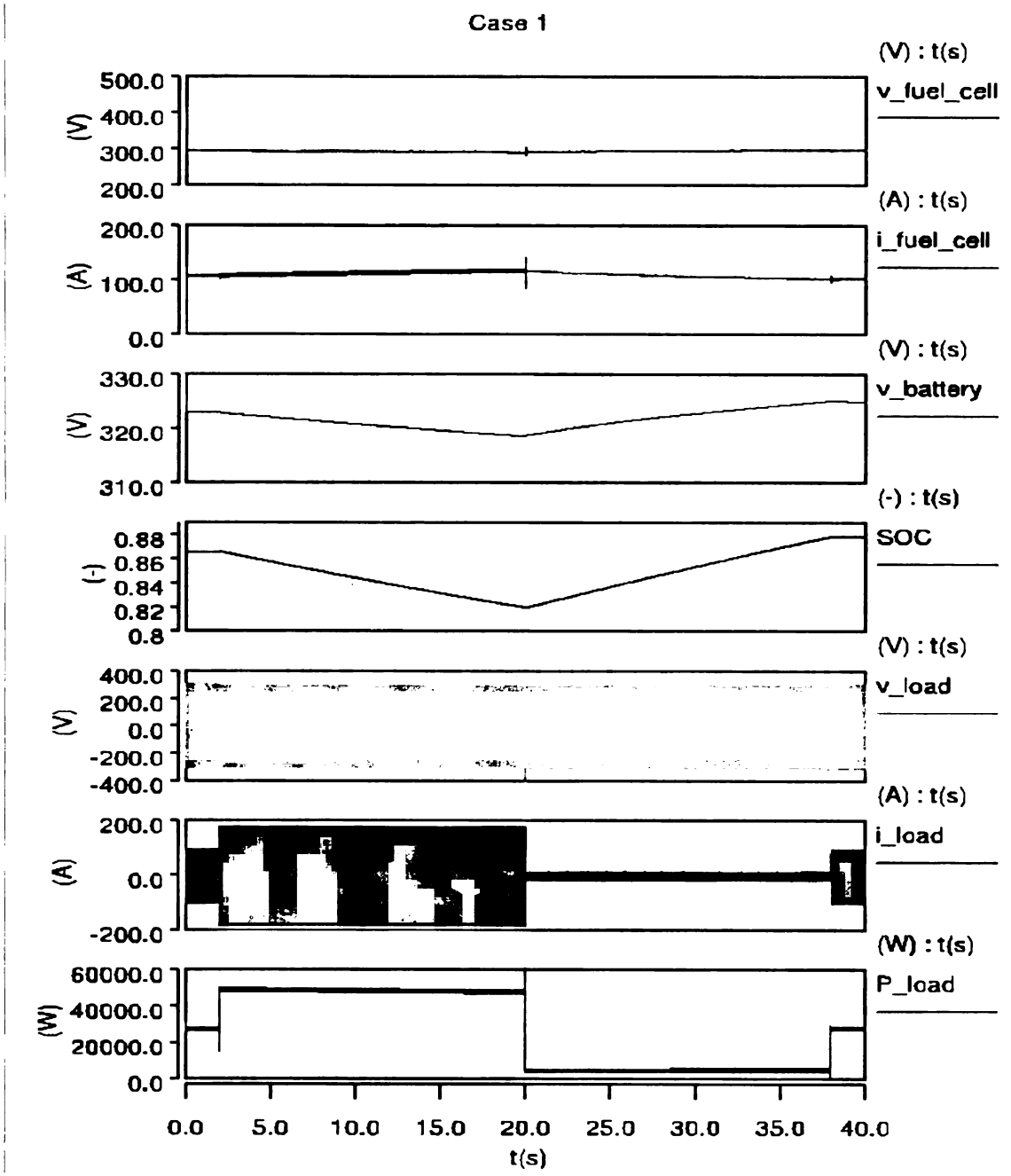

Figure 51. Simulation case 1

5.2.2 Simulation Case 2

The load power is kept constant at 30kW, and the fuel cell power is varied between 30kW, 50kW, 20kW. Again the battery SOC should remain constant while the fuel cell is producing 30kW. The battery will charge when the fuel cell power is increased to 50kW (Pin>Pout), increasing the SOC. When the fuel cell power is decreased to 20kW (Pin<Pout), the battery will supply the additional power requested by the load, decreasing the SOC.

This can be verified in Figure 52. Starting from the bottom, the load power, current, and voltage are constant, where the power is at approximately 30kW. Next are the battery SOC, battery voltage, fuel cell current, and fuel cell voltage. Initially the fuel cell produces 30kW, and the SOC stays constant. Then the fuel cell power is increased to 50kW and the SOC increases. Again the fuel cell produces 30kW, and the SOC stays constant. Next the fuel cell power is decreased to 20kW, and the SOC decreases. Finally, the fuel cell again produces 30kW, and the SOC stays constant.

Case 2 shows that we can control the fuel cell power, thus controlling the battery SOC. Case 2 also verifies the Z-source Inverter can be used to provide the medium, and high power operating modes. While the fuel cell is at 30kW the vehicle operates in the medium power mode, and while the fuel cell produces 50kW the vehicle operates in the medium power mode while charging the battery. When the fuel cell creates 20kW the vehicle is operating in the high power mode, as both the fuel cell and battery are providing power to the load.

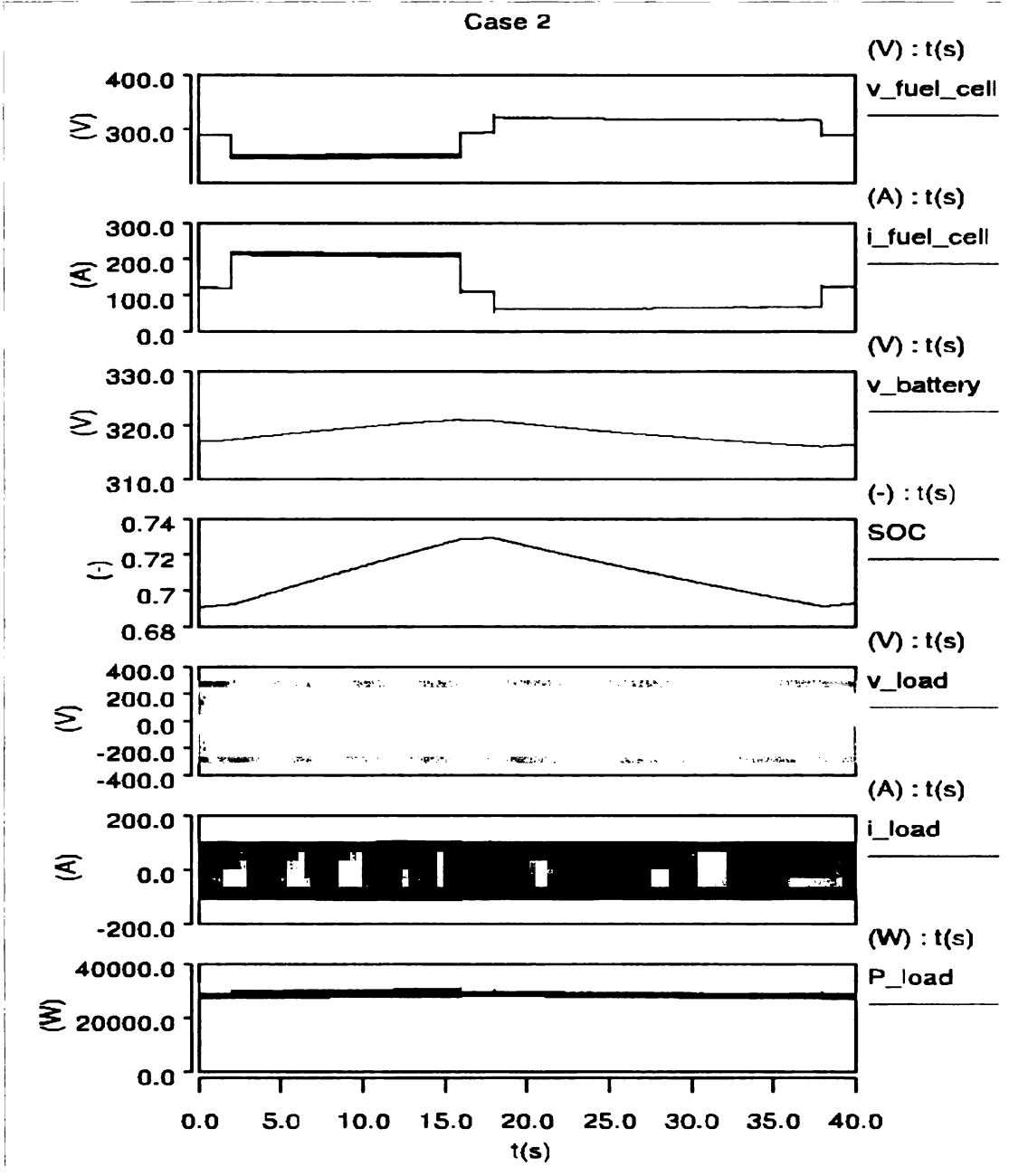

Figure 52. Simulation case 2

5.2.3 Simulation Case 3

The fuel cell operation is stopped, and the load power is varied from 5kW, to 20kW. As one would expect the battery SOC should decrease. These results are verified by simulation as seen in Figure 53, starting from the top, the fuel cell power is zero. Next are the battery voltage, SOC, load voltage, load current, and load power. Initially the load absorbs 5kW, and the SOC decreases slowly. The load is then increased to 20kW and the SOC decreases more rapidly. Case 3 verifies that the vehicle can be operated without using the fuel cell, strictly as an electric vehicle, as in the low power mode.

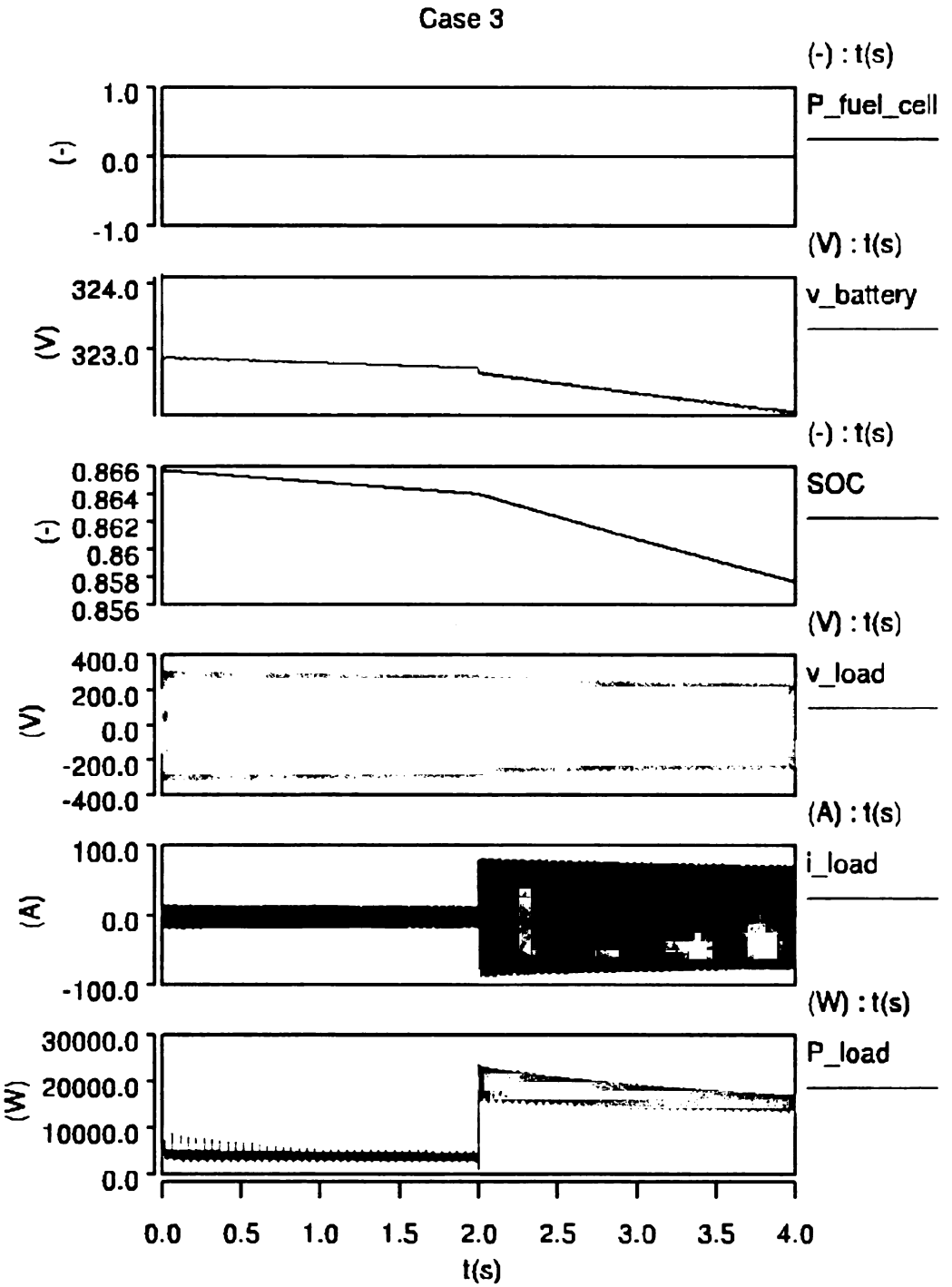

Figure 53. Simulation case 3

6. PROTOTYPE DEVELOPMENT, AND EXPERIMENTAL RESULTS

In this chapter experiments will be used to verify the Z-source inverter can be used to provide the above-mentioned hybrid system operating modes, control of battery SOC, control of fuel cell voltage (or power), and control of output voltage (or power). The experimental setup, as seen in Figure 54, will be discussed, including the fuel cell, battery, and load models. The experiment procedure is outlined, and the experimental results will be given.

6.1 Experimental Setup

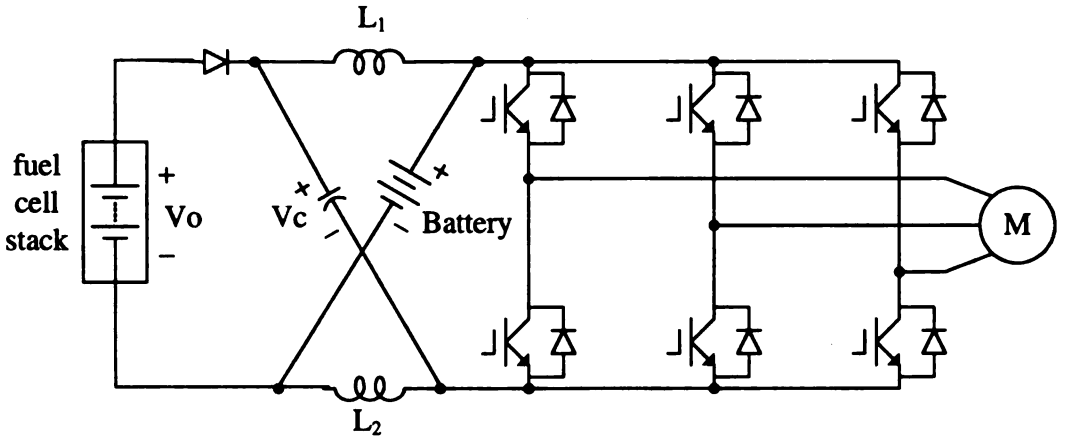

Figure 54. Schematic of experimental model

Figure 54 shows the schematic of the Zsource inverter to be used in a fuel cell vehicle. Before the experiments could be run, models of the fuel cell, battery, and load have to be developed.

6.1.1 Fuel Cell Stack

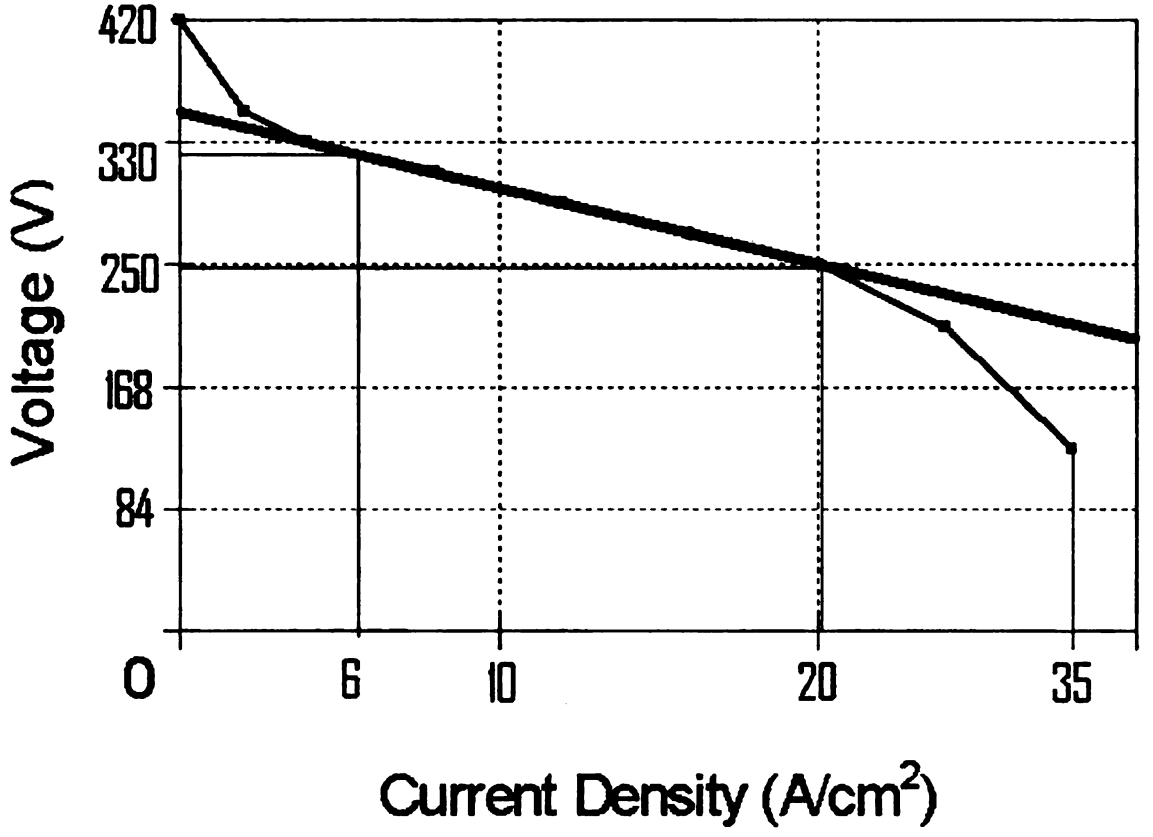

Figure 55. Linearized, scaled down, 5kW "Typical Fuel Cell Polarization Curve"

The fuel cell model was based on the "Typical Fuel Cell Polarization Curve" as seen previously. The polarization curve was linearized, as shown by the black line in Figure 55. The polarization curve was also scaled down to 5kW instead of 50kW, this was achieved by scaling down the current by a factor of ten. The reason the polarization curve was linearized was so a fuel cell model could be created from a dc voltage source in series with a resistor. The dc voltage source is set to the voltage at the Y-intercept, and the resistance is set to the slope of the line.

The problem with this approach is that the resistor required to achieve the desired

slope $R = \frac{\Delta X}{\Delta Y} = \frac{(330-250)}{(20-6)} = \frac{80}{14} = 5.714\Omega$ would consume too much power.

This problem is solved by selecting the resistance to be smaller, so less power is consumed. The resistance was chosen to be R=1.2Ω, because there were three 2kW .4Ω resistors available for use in our lab. The dc voltage source was randomly selected to be 250V, a lower voltage was desired for safety reasons.

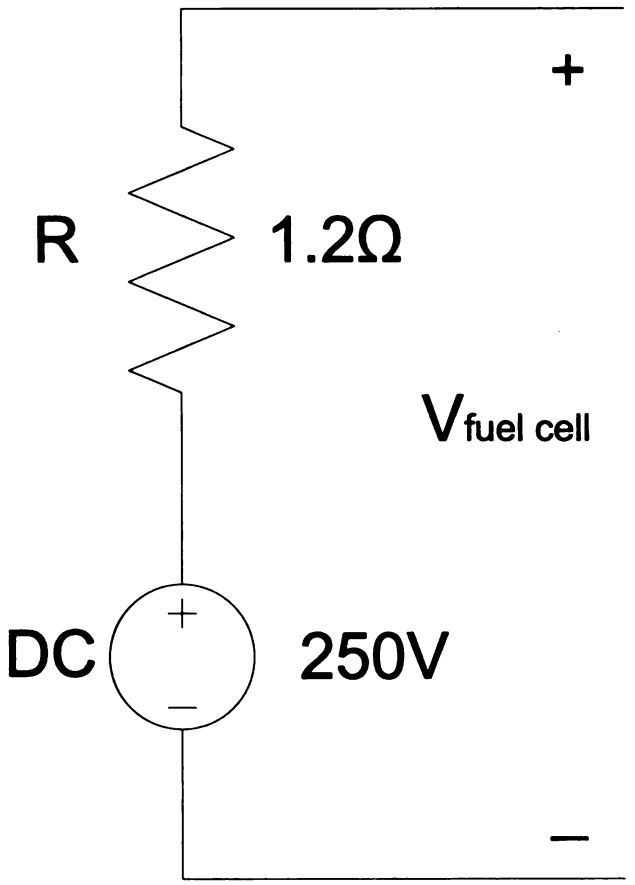

Figure 56. Experimental fuel cell model

The final fuel cell model schematic is shown in Figure 56. The model is created by connecting a 1.2 Ω resistor in series with a 250V dc voltage source.

The equation for voltage across the fuel cell produced by the final fuel cell model

is,

$$V_{fuel\_cell} = 250V - 1.2\Omega * I$$

Figure 57, shows the experimental fuel cell model polarization curve that was produced in SABER using the final fuel cell model. The approximate operating points used in the experiments are also shown in figure 57.

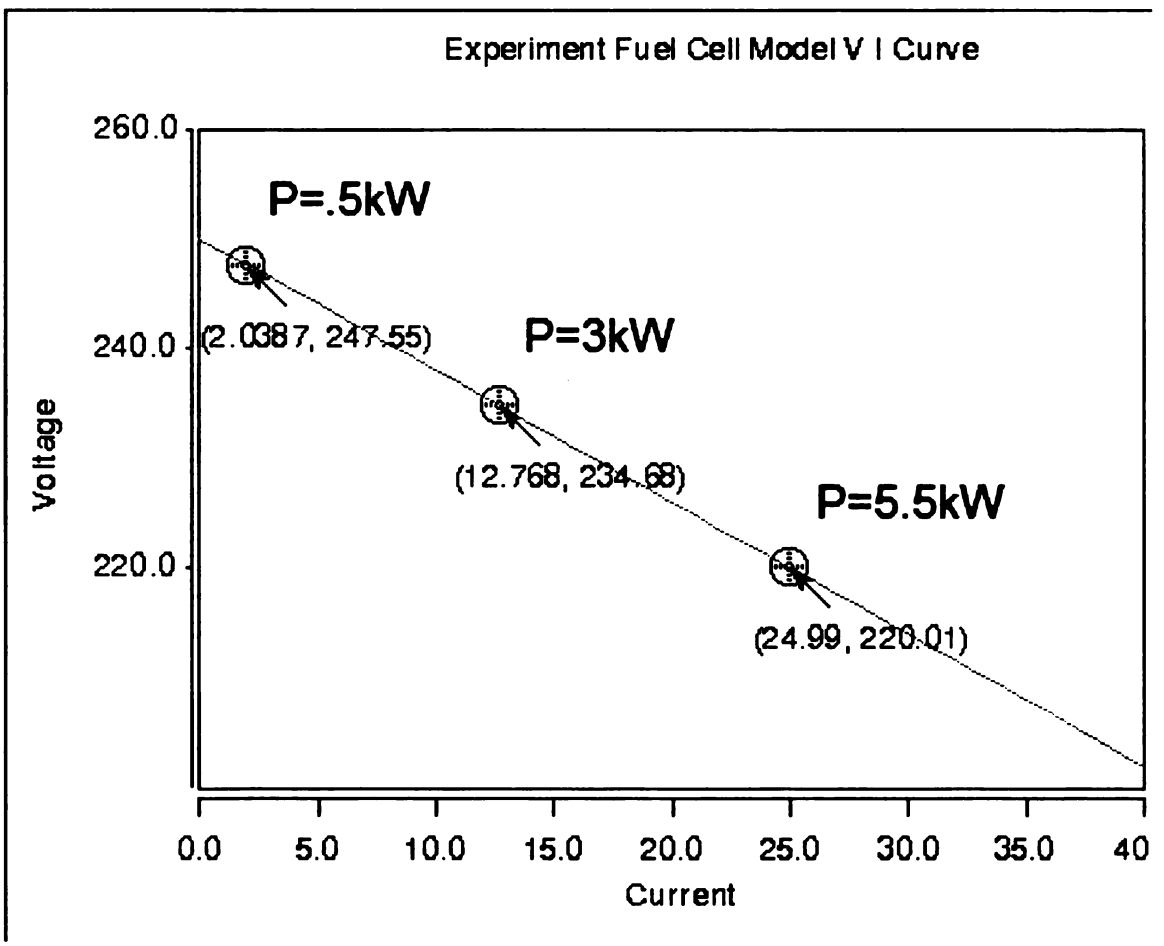

Figure 57. Experimental fuel cell model polarization curve

The final fuel cell model was constructed using the following technique. Three phase ac power was run through a circuit breaker then an isolation transformer, then a variable transformer was used to control the voltage level, this can be seen in Figure 58.

The voltage was then converted into dc using a three phase diode bridge rectifier, a 6mF capacitor is placed across the rectified dc voltage to smooth the ripple created by the rectifier, finally three .4Ω resistors, 1.2Ω total, were connected in series with the dc voltage, as can be seen in Figure 59.

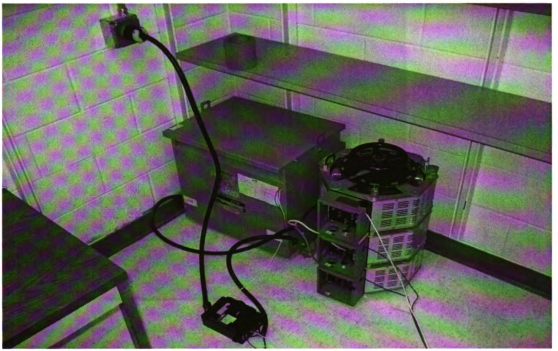

Figure 58. Three phase ac power, circuit breaker, isolation transformer, and variable transformer, were used to control the voltage level in the experiment

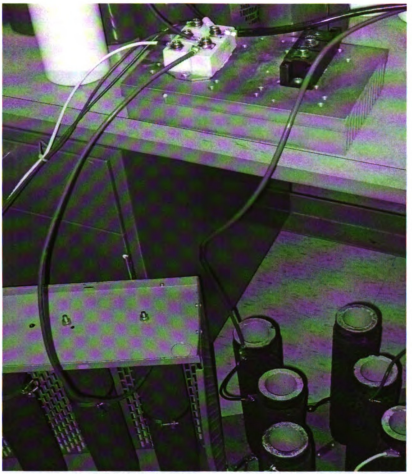

Figure 59. Three phase diode bridge rectifier, and 1.2Ω, were connected in series, to create the fuel cell model in the experiment

6.1.2 Battery

Figure 60. Capacitor bank used to replicate a battery in the experiments

Because there was no suitable high voltage battery available in our lab to be used in the experiments, a battery model was constructed using the following technique. As batteries and capacitors are both energy storing devices, a large capacitor bank can be used to replicate a battery. Figure 60 shows the capacitor bank used to replicate a battery in the experiments. The battery model consists of 25 6mF capacitors in parallel, in parallel with 8 5mF capacitors in parallel, for a total capacitance of 190mF.

6.1.3 Zsource Inverter

The 10kW Zsource inverter prototype shown in Figure 61 was used in the experiments. The circuit has the following parameters: Z-source network: L1 = L2 = 1 mH (60 Hz inductor), C1 = C2 = 1,300 μF (C2 is connected in parallel with the capacitor bank), and IGBTs are used for the switches.

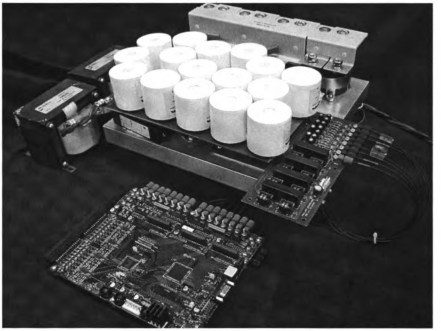

Figure 61. 10kW Zsource inverter prototype

6.1.4 Output Filter, and Load

The output filter and load (motor model), are the last pieces of the experimental setup to be discussed. Figure 62 shows their actual experimental setup. The low pass output filter is used to filter out the high frequency switching component of the output ac voltage. The components parameters are; the capacitors are 50μF wye connected, and the inductors are 1mH connected in series, giving a corner frequency of $fc = \frac{1}{\sqrt{LC}} = 4.47kHz$, which clearly will filter out the 10kHz switching frequency.

The load resistors were chosen based on the power requirements. Two 1kW 10Ω resistors were connected in parallel for each phase, giving each phase 2kW power rating and 5Ω, again the resistors are wye connected.

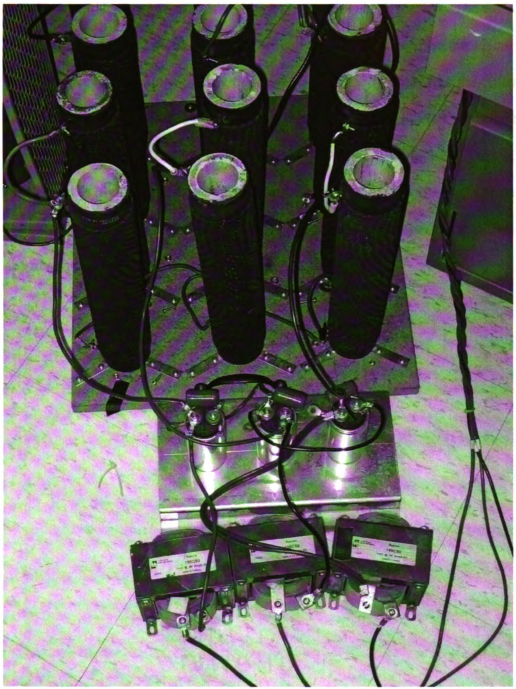

Figure 62. Output filter and load, used in the experiments

6.2 Experimental Results

6.2.1 Experiment Case 1

In the case 1 experiment the load power is varied from 3kW (M=.547, D_0=.179) to 5.5kW (M=.741, D_0=.179) to .5kW (M=.223, D_0=.179) back to 3kW. The fuel cell power is designed to 3kW constant, however fuel cell power varies because the 190mF capacitor bank can not store enough energy to handle the load dynamics, like the battery used in simulation would. Figure 63 shows that the battery can be used to handle the load dynamics, because the battery voltage varies with changes in the load. That is, when the load power is high the battery voltage drops because the battery is supplying power to the load, and when the load power is low the battery voltage increases because the battery absorbs the extra power from the fuel cell.

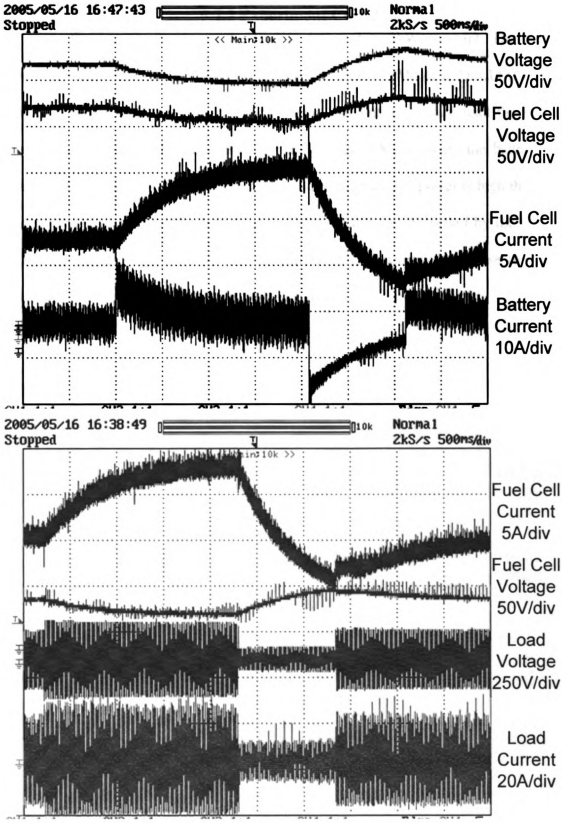

Figure 63. Experimental results case 1

6.2.2 Experiment Case 2

In the case 2 experiment the load is designed to 3kW constant. The fuel cell power is varied from 3kW (M=.556, D_0=.104) to 5.5kW (M=.487, D_0=.148) to .5kW (M=.645, D_0=0) back to 3kW. Figure 64 shows that under constant load the fuel cell power can be controlled, thus controlling the battery SOC, allowing the battery to be charged, discharged or held constant. That is, when the fuel cell power is high the battery voltage increases because the battery absorbs the excess power created by the fuel cell, and when the fuel cell power is low the battery voltage decreases because the battery must supply the excess power requested by the load.

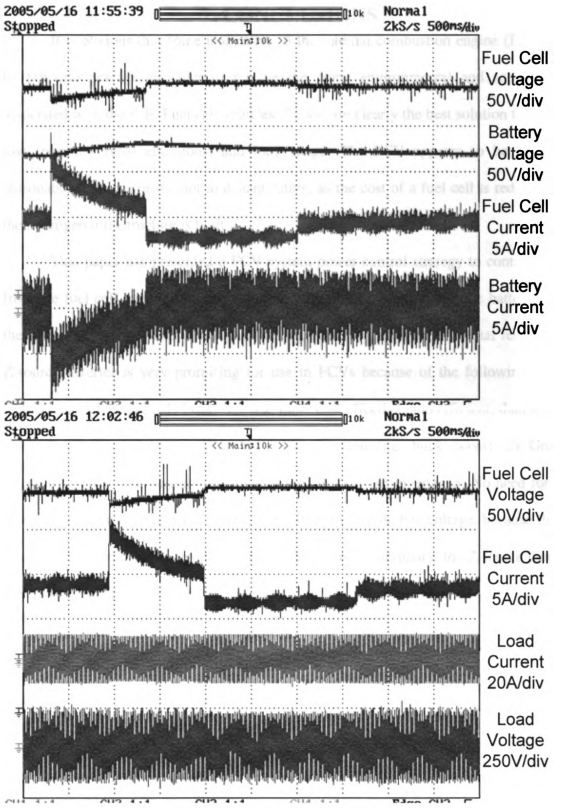

Figure 64. Experimental results case 2

7. CONCLUSIONS

It is obvious that some alternative to the internal combustion engine (ICE) must be put into practice in order to resolve the many environmental and social issues associated with the ICE. Fuel cell vehicles (FCVs) are clearly the best solution to provide low (possibly zero) emissions, and long range. The FCV appears to be the most reasonable solution for the not to distant future, as the cost of a fuel cell is reduced, and the hydrogen infrastructure is built.

This paper has presented a FCV system power control strategy to control power from the fuel cell, power to the motor, and State of Charge (SOC) of the battery, using the Z-source inverter. This is also verified by simulation, and experimental results. The Z-source inverter is very promising for use in FCVs because of the following unique features and advantages: 1) Less complex, more cost effective, and efficient, than a dc-dc boosted inverter, while providing the same function (i.e. buck boost). 2) Greater reliability, because shoot-through can no longer destroy the inverter. 3) No need for any dc-dc converters to control the battery SOC, or boost the dc bus voltage, because the Z-source inverter has two independent control freedoms. In summary, the Z source inverter is very promising for fuel cell vehicles.

REFERENCES

[1] S Pischinger; O Lang; H Kemper; "System Comparison of Hybrid and Fuel Cell Systems to Internal Combustion Engines," SAE 2002 technical paper series, October 2002, Ref: 2002-21-0070.

[2] J Contadini; "Social Cost Comparison Among Fuel Cell Vehicle Alternatives," American Institute of Aeronautics and Astronautics, Inc. 2000, Ref: AIAA-2000-3043.

[3] D Sperling; *Future Drive*. Washington, D.C.: Island Press, 1995.

[4] M.J. Bradley, and Associates; *Report 59 Hybrid-Electric Transit Buses: Status, Issues, and Benefits.* Washington, D.C.: National Academy Press, 2000.

[5] H. Moghbelli, K. Ganapavarapu, and R. Langari, "A comparative review of fuel cell vehicles (FCVs) and hybrid electric vehicles (HEVs) – Part II," in *Proc. SAE Future Transportation Technology Conf.,* Costa Mesa, CA, June 2003.

[6] National Research Council, and National Academy of Engineering; *The Hydrogen Economy.* Washington, D.C.: National Academy Press, 2004.

[7] R. Thring; *Fuel Cells for Automotive Applications.* New York, NY: The Americal Society of Mechanical Engineers, 2004.

[8] K. Thorborg; *Power Electronics*. London, U.K.: Prentice-Hall International (U.K.) Ltd., 1988.

[9] F. Z. Peng, "Z-Source Inverter," IEEE Transactions on Industry Applications, vol. 39, No. 2, pp. 504-510, March/April 2003.

[10] A. Emadi, S. S. Williamson; "Fuel Cell Vehicles: Opportunities and Challenges," Grainger Power Electronics and Motor Drives Laboratory, Electric Power and Power Electronics Center, Illinois Institute of Technology, Chicago, IL, http://www.ece.iit.edu/~emadi/

[11] M.H. Rashid; *Power Electronics*, 2nd ed. Englewood Cliffs, NJ: Prentice-Hall, 1993.

[12] R. Erickson, D. Maksimovic; *Fundamentals of Power Electronics,* 2nd ed. Norwell, MA: Kluwer Academic Publishers, 2001.

[13] G. Ledwich, "Pulse Width Modulation (PWM) Basics," website, 1998. http://www.powerdesigners.com/InfoWeb/design_center/articles/PWM/pwm.shtm

[14] V. Onde; " ST92141 AC Motor Control Software Library Version 2.1 Update," AN1367 Application Note, STMicroelectronics, 2002.

[15] D.A. Grant and J. A. Houldsworth: PWM AC Motor Drive Employing Ultrasonic Carrier. *IEE Conf. PE-VSD*, London, 1984, pp. 234-240.

[16] F. Z. Peng and Miaosen Shen, Zhaoming Qian, "Maximum Boost Control of the Z-source Inverter," in *Proc. of IEEE PESC 2004.*

[17] Miaosen Shen, Jin Wang, Alan Joseph, Fang Z. Peng, Leon M. Tolbert, and Donald J. Adams, "Maximum constant boost control of the Z source inverter." in Proc. IEEE IAS'04, 2004, p.142.

[18] Miaosen Shen, Alan Joseph, Jin Wang ,Fang Z. Peng, and Donald J. Adams, "Comparison of Traditional Inverters and Z-Source Inverter for Fuel Cell Vehicles," in Proc. IEEE Power Electronics in Transportation, October 2004, Novi, MI, p. 125.

[19] K. Rajashekara, "Power Conversion and Control Strategies for Fuel Cell Vehicles," in Proc. Industrial Electronics Society, 2003, vol. 3, pp. 2865- 2870.

[20] Tadaichi Matsumoto; Nobuo Watanabe; Hiroshi Sugiura; Tetsuhiro Ishikawa; "Development of Fuel-Cell Hybrid Vehicle," Fuel cell power for transportation 2002 conference, SAE 2002 World congress, March 2000, Ref: 2002-01-0096

[21] B. D'Souza, H. Rawlins, J. Machuca, C. Larson, M. Shuck, B. Shaffer, T. Maxwell, M. Parten, D. Vines, and J. Jones, "Texas Tech University Developes Fuel Cell Powered Hybrid Electric Vehicle for FutureCar Challenge 1998," SAE 1999, Ref: 1999-01-0612.

[22] J. Adams, W. Yang, K. Oglesby, and K. Osborne, "The Development of Ford's P2000 Fuel Cell Vehicle," SAE 2000, Ref: 2000-01-1061.

[23] D. Tran, and M. Cummins, "Development of the Jeep Commander 2 Fuel Cell Hybrid Electric Vehicle," SAE 2001, Ref: 2001-01-2508.

[24] Synopsys, "Saber Mixed-Technology," website, 2005.
http://www.synopsys.com/home.html

[25] Pukrushpan, Jay T., Stefanopoulou, Anna G., Peng, Huei, "Modeling and Analysis of Fuel Cell Reactant Flow for Automotive Applications," in Journal of Dynamic Systems, Measurement and Control, 126 (1), pp. 14-25, March 2004.

[26] E. H. Wakefield; *History of the Electric Automobile,* Warrendale, PA: Society of Automotive Engineers, Inc, 1998.

[27] H. Park, C. Han, C. Kim, B. Lee, Y. Kim, and P. Gifford, "Ni-MH Battery Charger with a Compensator for Electric Vehicles," in Proc. SAE Strategies in Electric and Hybrid Vehicle Design, 1996 SAE International Congress and Exposition, 1996, p. 125.